Geological Magazine

www.cambridge.org/geo

A revised palynozonation for the Middle–Upper Triassic (Anisian–Rhaetian) Series of the Norwegian Arctic

Niall William Paterson[1,2] and Gunn Mangerud[1]

[1]Department of Earth Science, University of Bergen, Post box 7803, N-5020 Bergen, Norway and [2]CASP, West Building, Madingley Rise, Cambridge, CB3 0UD, United Kingdom

Original Article

Cite this article: Paterson NW and Mangerud G (2020) A revised palynozonation for the Middle–Upper Triassic (Anisian–Rhaetian) Series of the Norwegian Arctic. *Geological Magazine* **157**: 1568–1592. https://doi.org/10.1017/S0016756819000906

Received: 28 February 2019
Revised: 17 June 2019
Accepted: 11 July 2019
First published online: 14 November 2019

Keywords:
Triassic; palynology; zonation; Svalbard; Barents Sea

Author for correspondence:
Niall William Paterson,
Email: niall.paterson@casp.org.uk

Abstract

The Barents Sea region of Arctic Norway preserves a thick succession of marine and deltaic Triassic strata that yield an abundant and diverse association of terrestrial and marine palynomorphs. Despite being the principal means for dating and correlation across this vast region, the Upper Triassic palynozonal resolution has remained relatively low. This is problematic due to the thickness of the Upper Triassic Series and since this corresponds to the longest of the three Triassic epochs. This paper presents a refined Middle–Upper Triassic palynozonation for the region, based on a detailed investigation of multiple localities ranging from the Svalbard Archipelago to the southern Barents Sea. The zonation comprises eleven spore-pollen zones: the *Carnisporites spiniger*, *Triadispora obscura* and *Protodiploxypinus decus* zones (Anisian), the *Echinitosporites iliacoides* Zone (Ladinian), the *Semiretisporis hochulii*, *Podosporites vigraniae*, *Leschikisporis aduncus*, and *Protodiploxypinus* spp. zones (Carnian), the *Classopollis torosus*, and *Quadraeculina anellaeformis* zones (Norian), and the *Ricciisporites* spp. Zone (Rhaetian). Additionally, two new dinoflagellate cyst zones are defined: the *Rhaetogonyaulax arctica* (upper Carnian – lower Norian) and *Rhaetogonyaulax rhaetica* (lower Norian) zones. Three new age-significant palynomorph taxa are described: *Kyrtomisporis moerki* sp. nov., *Podosporites vigraniae* sp. nov. and *Semiretisporis hochulii* sp. nov. The revised palynozonation is compared with previous palynozonal schemes for the Greater Barents Sea region, and its relationship to Triassic palaeoclimate, palaeoenvironments and sequence stratigraphy is discussed.

1. Introduction

The Barents Shelf and adjacent Svalbard, Franz Josef Land and Novaya Zemlya archipelagos (Fig. 1) preserve a near-continuous succession of Triassic strata that were deposited in a long-lasting intracratonic basin (Sømme *et al.* 2018). In contrast to arid-terrestrial and carbonate deposits typifying 'classical' Triassic localities of the Germanic and Alpine realms, the Triassic strata of the Barents Sea reflect a range of deltaic and shallow-marine palaeoenvironments from a warm-temperate palaeoclimatic belt along the northern coast of Pangaea (Boucot *et al.* 2013).

Following the discovery of hydrocarbons in the Norwegian Barents Sea in the early 1980s, palynostratigraphy has become an essential tool for the dating of Triassic strata in the region, leading to the description of palynozonal schemes by Hochuli *et al.* (1989) and Vigran *et al.* (2014). Nonetheless, Late Triassic zonal resolution remains relatively low, with only four zones established for an interval spanning approximately 36 Ma (Ogg *et al.* 2016). The absence of a high-resolution Upper Triassic palynostratigraphy was the motivation for a series of studies focused on the Middle–Upper Triassic (Anisian–Rhaetian) stratigraphy of Svalbard and the Norwegian Barents Sea by the current authors (Paterson & Mangerud, 2015, 2017; Paterson *et al.* 2016, 2017, 2019*a*). Collectively, these form the basis of a refined palynozonal scheme that is presented in Section 3 (Revised zonal scheme).

The Late Triassic palaeoclimate was characterized by prevailing aridity in many regions, particularly in central Pangaean localities, but this was briefly interrupted by humid conditions during the Carnian Pluvial Episode (Simms & Ruffell, 1989, 2018; Simms *et al.* 1994; Ruffell *et al.* 2015). Intriguingly, the epoch was also important in terms of biotic development on land and in the ocean, with the origination and diversification of several new groups including dinosaurs, lizards, mammals, calcareous nannoplankton and dinoflagellate cysts (Furin *et al.* 2006; Benton *et al.* 2018; Bernardi *et al.* 2018; Mangerud *et al.* 2018). Since plant distribution is largely controlled by climate, a more detailed record of the palynofloral succession from the Barents Sea region contributes to our understanding of the impact of such climatic perturbations on the biotas of northern Pangaea.

Collectively, the data gathered by previous studies has revealed that substantial differences exist between the Late Triassic palynofloras in the Barents Sea region compared with those

CAMBRIDGE UNIVERSITY PRESS

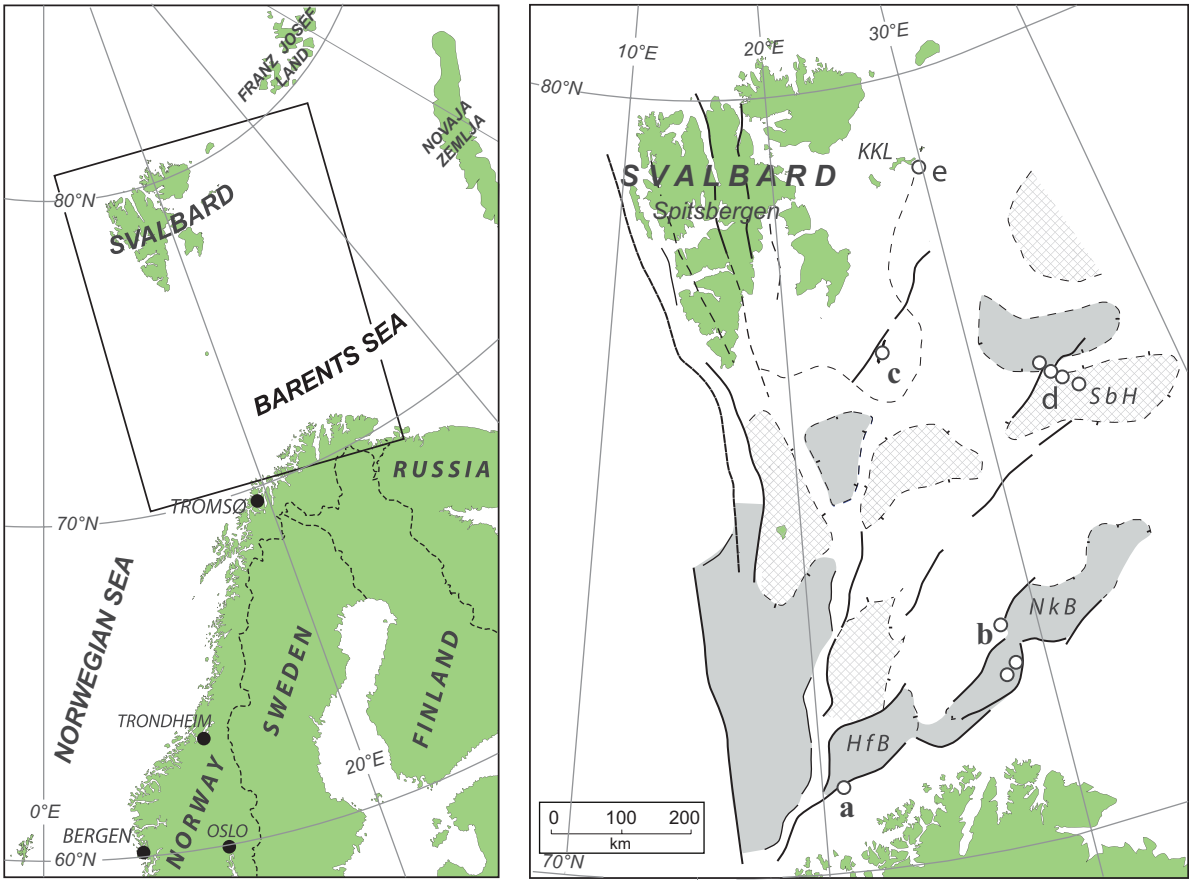

Fig. 1. Geological and structural map of Svalbard and the Barents Sea (after Vigran *et al.* 2014; simplified from Dallmann, 1999). Reference localities: a, exploration wells 7120/12-2; b, 7228/2-1s, 7-1a and 9-1s; c, Hopen; d, stratigraphic boreholes 7533/2-U-1, 2-U-2 and 3-U-7, and 7534/4-U-1; e, boreholes 7830/3-U-1, 5-U-1, 6-U-1, and 7831/2-U-1 and 2-U-2. HfB – Hammerfest Basin; NkB – Nordkapp Basin; SbH – Sentralbanken High; KKL – Kong Karls Land.

described from central and southern European localities. Such differences likely reflect palaeoclimatic control across a palaeolatitudinal gradient (Hochuli & Vigran, 2010; Vigran *et al.* 2014). Since independent age control indicates that many palynomorph index taxa have significantly earlier first occurrences in the Greater Barents Sea area (Smith, 1982; Hochuli *et al.* 1989; Hochuli & Vigran, 2010; Paterson & Mangerud, 2015; Paterson *et al.* 2019*a*), it appears the humid coastal region of northern Pangaea was a 'cradle' for floristic evolution during Late Triassic time. Refinement of existing palynozonation is therefore not only important for regional stratigraphic correlations, but is also critical for understanding the timing and drivers for the origination and dispersal of Late Triassic floras.

2. Geological background

2.a. Lithostratigraphy

The Triassic succession in the Barents Sea region primarily comprises siliciclastic deposits reflecting a suite of coastal plain, deltaic, prodeltaic and restricted marine palaeoenvironments. Seismic data show these as NW-prograding clinoform packages that define a series of seismic sequences (Riis *et al.* 2008; Glørstad-Clark *et al.* 2010, 2011; Høy & Lundschien, 2011; Klausen *et al.* 2015). Following the catastrophic destruction of long-lasting carbonate platform environments during the Permian–Triassic mass extinction, siliciclastic deposits derived principally from the Polar Urals and Fennoscandia rapidly filled the basin, prograding as far as the Svalbard Archipelago by the Carnian Age (Lundschien *et al.* 2014; Eide *et al.* 2018; Sømme *et al.* 2018). The progradation of deltaic systems during the Triassic Period likely played an important role in the floristic development of the region because, by the late Carnian Age, it had led to the establishment of a vast area of coastal plain and marginal marine habitats (Paterson *et al.* 2016; Klausen *et al.* 2019).

The lithostratigraphic scheme for the region outlined by Mørk *et al.* (1999) divides the succession into two groups: the Sassendalen Group (Changhsingian/Induan–Anisian) and the Kapp Toscana Group (Ladinian – Middle Jurassic) (Fig. 2). The Sassendalen Group comprises the Havert (Changhsingian–Olenekian), Klappmyss (Olenekian) and Kobbe (Anisian) formations; organic-rich mudrocks of the Steinkobbe Formation are correlative (in part) to the latter. The Triassic portion of the Kapp Toscana Group includes the Snadd (Ladinian – upper Carnian), Fruholmen (upper Carnian – Rhaetian) and Tubåen (Rhaetian–Hettangian) formations. The sequence stratigraphy of the Triassic deposits on the Norwegian Barents Shelf has been described by a series of studies (including Riis *et al.* 2008; Glørstad-Clark *et al.* 2010, 2011; Høy & Lundschien, 2011; Klausen *et al.* 2015), with six second-order and eighteen third-order sequences delineated by regionally extensive maximum flooding surfaces (Fig. 3). Fluctuations in relative sea level during the Triassic Period likely influenced palynofloral development in the region as coastal habitats were periodically created and lost (Paterson *et al.* 2016).

https://doi.org/10.1017/S0016756819000906 Published online by Cambridge University Press

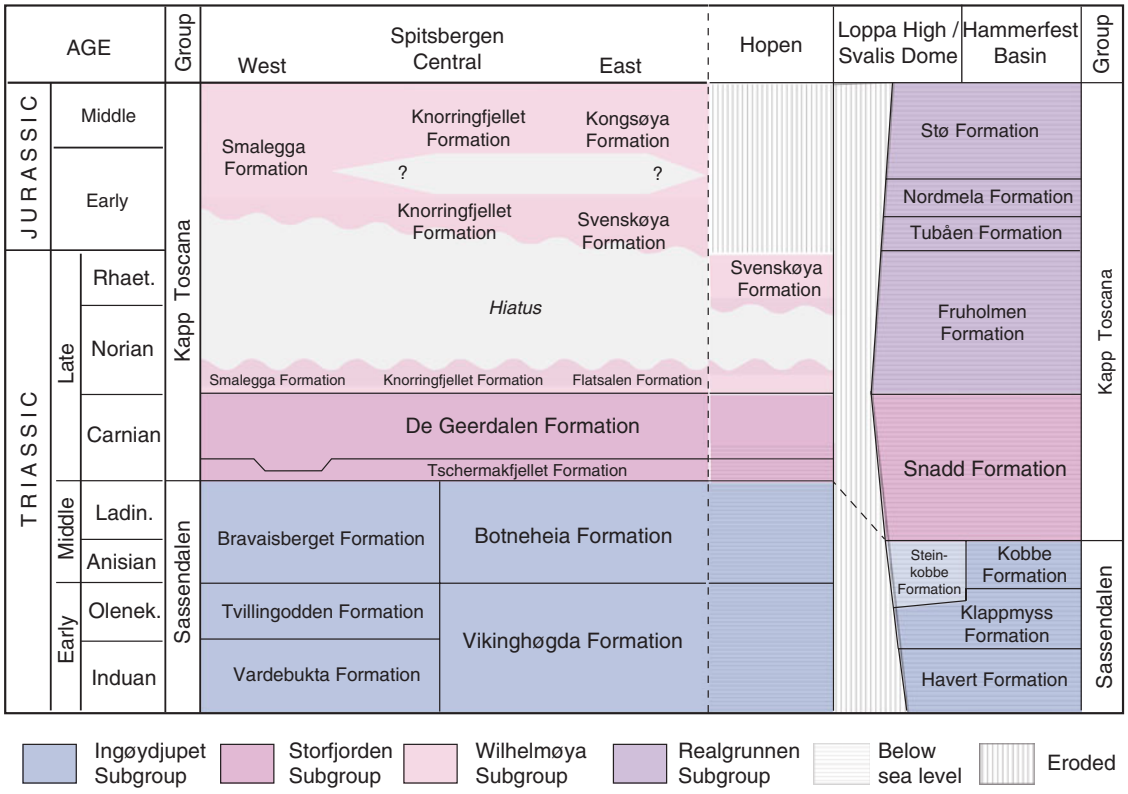

Fig. 2. Lithostratigraphical scheme for the Triassic and Lower–Middle Jurassic strata on Svalbard and in the subsurface Norwegian Barents Shelf. Modified from Mørk *et al.* (1999).

As on the Barents Shelf, the Triassic succession on Svalbard is assigned to the Sassendalen and Kapp Toscana groups (Fig. 2). However, due to diachroneity resulting from the SE–NW progradation of the strata, the boundary between the groups is younger than in the subsurface Barents Sea, and corresponds approximately to the Middle–Upper Triassic (Ladinian–Carnian) boundary. On Svalbard, the groups are subdivided into an alternative series of local formations, which in the eastern parts of the archipelago comprise the Vikinghøgda and Botneheia formations (Sassendalen Group) and the Tschermakfjellet, De Geerdalen, Flatsalen and Svenskøya formations (Kapp Toscana Group) (Fig. 2).

2.b. Previous palynological schemes

The initial palynostratigraphic studies of Triassic strata in the region focused on outcrops of the Kapp Toscana Group on Hopen, Kong Karls Land and central Spitsbergen (e.g. Smith, 1974; Smith *et al.* 1975; Bjærke, 1977; Bjærke & Dypvik, 1977; Bjærke & Manum, 1977). The first of these (Smith, 1974) described assemblages from the Iversenfjellet Formation (now De Geerdalen Formation) on Hopen that were tentatively dated as Carnian–Rhaetian. A subsequent study of the island by Smith *et al.* (1975) and Bjærke & Manum (1977) considered the assemblages as being of Carnian – Early Jurassic and Rhaetian age, respectively, based on the limited independent dating evidence available at that time, and by comparison with the ranges of key taxa from central and southern Europe. However, an early Norian ammonoid fauna (kerri Zone) later described from the Flatsalen Formation (Korčinskaya, 1980) prompted a reconsideration of the age of the palynofloras. The implications of the ammonoid dating were discussed by Smith (1982) who recognized that many typically 'Rhaetian' taxa had surprisingly early first occurrences in the Barents Sea region.

Consequently, recent studies in the region have relied less on interregional correlation, seeking instead to establish a regional zonation, calibrated to the global timescale by independent age constraints. The palynozonation of Hochuli *et al.* (1989) comprises 15 'assemblages' (named A–P) spanning the Triassic Period (Fig. 3). This includes four Early Triassic assemblages: P (Griesbachian, ? early Griesbachian), O (Dienerian–Griesbachian), N (Smithian) and M (Spathian); five Middle Triassic assemblages: L (early Anisian), K (late Anisian), I (early Ladinian), H ('middle' – late Ladinian) and G (late Ladinian, now redated as early Carnian); and six Late Triassic assemblages: F (early Carnian), E and D ('middle' Carnian), C (late Carnian), B-1 and B-2 (Norian and Norian–Rhaetian, respectively), and A (Rhaetian).

The palynozonation of Vigran *et al.* (2014) defined 15 formalized composite assemblage zones ranging from the Changhsingian to Rhaetian (Fig. 3). This zonation has particularly high resolution in the uppermost Permian and Lower Triassic strata, where seven ammonoid calibrated zones are defined: the *Uvaesporites imperialis* (Changhsingian), *Reduviasporonites chalastus* (uppermost Changhsingian – lower Griesbachian), *Proprisporites pocockii* (upper Griesbachian), *Maculatasporites* spp. (Dienerian), *Naumovaspora striata* (Smithian), *Pechorosporites disertus* (lower Spathian) and *Jerseyiaspora punctispinosa* (upper Spathian) zones. The Middle and the Upper Triassic strata are both represented by four zones each: the *Anapiculatisporites spiniger* (lower Anisian), *Triadispora obscura* (middle Anisian), *Protodiploxypinus decus* (upper Anisian) and *Echinitosporites iliacoides* (Ladinian) zones; and the *Aulisporites astigmosus* (lower–'middle' Carnian), *Rhaetogonyaulax* spp. (upper Carnian), *Limbosporites lundbladii*

https://doi.org/10.1017/S0016756819000906 Published online by Cambridge University Press

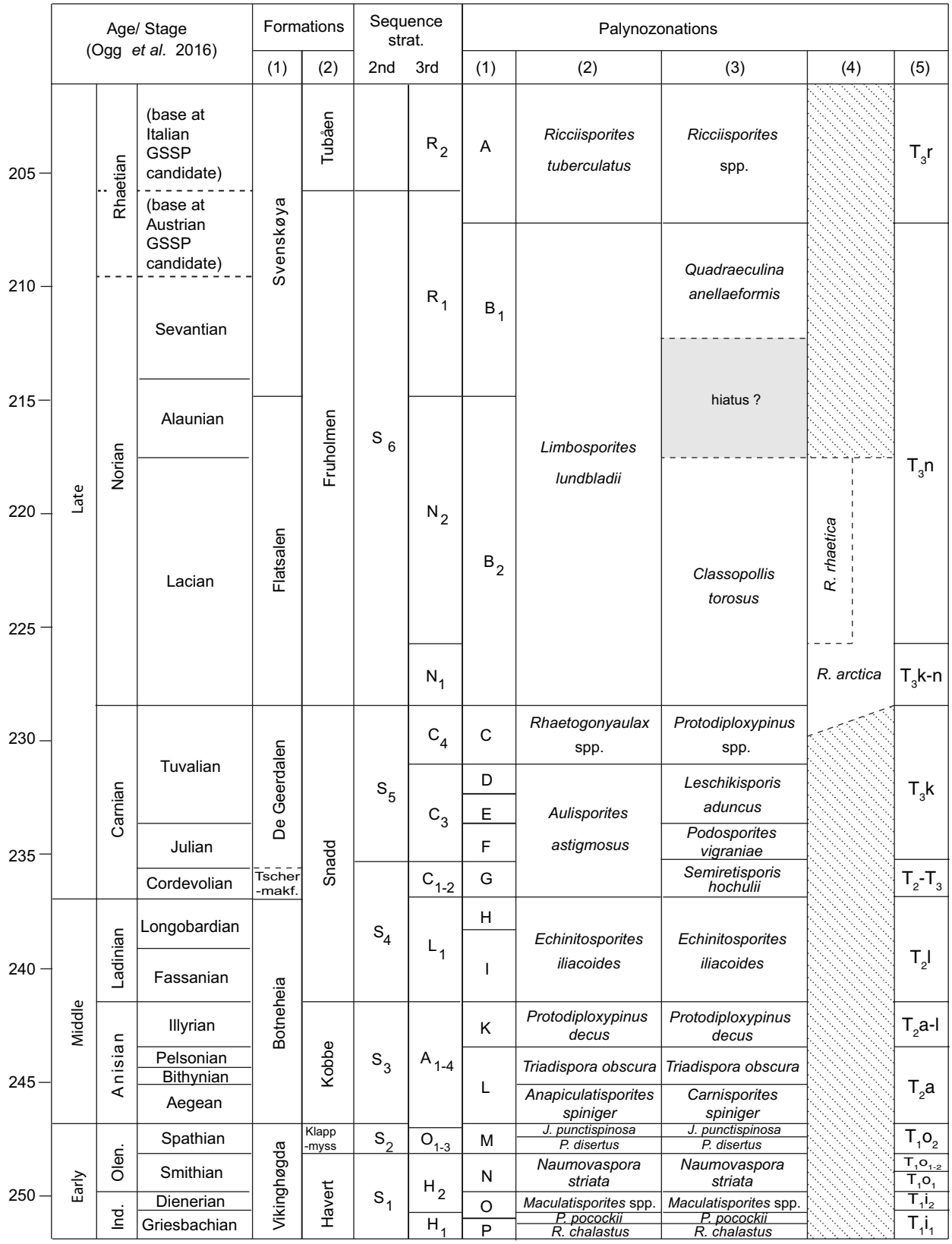

Fig. 3. Spore-pollen zonal schemes for the Lower–Upper Triassic (Induan–Rhaetian) succession of Svalbard and the Barents Shelf: (1) Hochuli *et al.* (1989); (2) Vigran *et al.* (2014); (3) this study; and (5) Fefilova (2001). (4) Dinoflagellate cyst zones, this study. Timescale after Ogg *et al.* (2016). Formations from (1) eastern Svalbard and (2) Norwegian Barents Shelf. Second- and third-order stratigraphic sequences from Glørstad-Clark *et al.* (2010) and Klausen *et al.* (2015).

https://doi.org/10.1017/S0016756819000906 Published online by Cambridge University Press

(Norian) and *Ricciisporites tuberculatus* (Rhaetian) zones. However, despite the improved Lower Triassic resolution, a significant limitation of the zonation is the relatively low Upper Triassic resolution.

In order to increase the Upper Triassic zonal resolution, we outlined a series of palynological assemblages for the Upper Triassic strata on Svalbard and in stratigraphical cores and exploration wells from the southern Barents Sea (Paterson & Mangerud, 2015, 2017; Paterson *et al.* 2016, 2017, 2019*a*, *b*). These assemblages were originally defined as informal biostratigraphic subdivisions since it was suspected that their temporal and geographical distribution might be facies dependent. However, since comparable assemblages have now been consistently recognized in correlative deposits throughout the region by us and other authors (e.g. Mueller *et al.* 2016; Rismyhr *et al.* 2018; Smelror *et al.* 2019), they are now confidently elevated to full zonal status.

3. Revised zonal scheme

The present Anisian–Rhaetian spore-pollen zonation comprises 11 composite assemblage zones (Figs 3, 4a, b), referred to here as 'zones'. Additionally, two dinoflagellate cyst zones are defined for the late Carnian (Tuvalian) – early Norian (Lacian) ages. Biostratigraphic events used in the recognition of the zones are defined in Table 1. Representative palynomorph taxa for the zones are illustrated in Figures 5–10.

The Middle Triassic (Anisian and Ladinian) zonation is essentially unmodified from Vigran *et al.* (2014). However, the early Anisian *Anapiculatisporites spiniger* Zone is renamed here as the *Carnisporites spiniger* Zone to reflect the revised taxonomy of Morbey (1975). Each of the zones is described in the following subsections and correlated with previous palynozonal schemes (Fig. 3). The early Carnian *Semiretisporis hochulii* and the *Podosporites vigraniae* zones are named after newly defined taxa, which are described in Section 5 (Systematic palynology) together with a third taxon, *Kyrtomisporis moerki* sp. nov. The new species are illustrated in Figures 5, 6 and 11. All palynomorph specimens shown in Figures 5–11 are curated in the palaeontological collections of the Natural History Museum, Oslo (except for some of those illustrated in Fig. 10, which belong to Applied Petroleum Technology, Oslo).

3.a. Anisian

3.a.1. Carnisporites spiniger Zone

Definition: The base of the *Carnisporites spiniger* Zone is defined by the consistent first occurrences of *Carnisporites spiniger*, *Illinites chitonoides* and *Podosporites amicus* (Vigran *et al.* 2014, p. 70) and the first occurrences of *Falcisporites stabilis*, *Kuglerina meieri* and *Staurosaccites quadrifidus* (Fig. 4a). The base of the zone also coincides with the last occurrence of *Crustaesporites globosus*.

Biozonal assemblages: The zone is characterized by the common to abundant occurrence of *Aratrisporites* spp., together with the common occurrence of *Jerseyiaspora punctispinosa* and various species of *Triadispora*.

Occurrence: On Svalbard, assemblages assigned to the *Carnisporites spiniger* Zone have been recorded in the Bravaisberget Formation (Passhatten Member) and in the equivalent Botneheia Formation (Muen Member) (Fig. 2), in association with ammonoids of the lower Anisian *Karangites evolutus* Zone (Vigran *et al.* 2014). The zone is also recorded in the correlative Steinkobbe Formation in shallow stratigraphical core 7323/7-U-4 from the Svalis Dome, and in the Kobbe Formation in several exploration wells from the Hammerfest, Maud and Nordkapp basins (Vigran *et al.* 2014; Paterson & Mangerud, 2017).

Biostratigraphic correlation: According to Vigran *et al.* (2014, fig. 3a), the lower part of the *Carnisporites spiniger* Zone corresponds to the *Striatella seebergensis* – *Accinctisporites circumdatus* – *Anapiculatisporites spiniger* – *Pretricolpipollenites* spp. Concurrent Range Zone ('Svalis-5') of Vigran *et al.* (1998) described from the Steinkobbe Formation on the Svalis Dome. The zone correlates with 'Assemblage L' of Hochuli *et al.* (1989), and to 'floral phases 3 and 4' of Hochuli & Vigran (2010). Comparable assemblages rich in *Aratrisporites* spp. have also been recorded from the Anisian 'T_2a palynocomplex' of the Russian Barents Sea (Pavlov *et al.* 1985; Mørk *et al.* 1993; Fefilova, 2013) (Fig. 3).

Age: The zone is dated as early Anisian by the co-occurrence of an ammonoid fauna assigned to the *Karangatites evolutus* Zone on Svalbard and in shallow stratigraphic core 7323/07-U-04 from the Svalis Dome (Weitschat & Dagys, 1989; Vigran *et al.* 1998, 2014).

3.a.2. Triadispora obscura Zone

Definition: The *Triadispora obscura* Zone was defined by Vigran *et al.* (2014, p. 71) with the zone base coinciding with the last occurrence of *Densoisporites nejburgii*, and by the first occurrences of *Camarozonosporites laevigatus*, *Protodiploxypinus minor*, *P. ornatus* and *Pseudoenzonalasporites summus*. The top of the zone is defined by the last consistent occurrence of *Jerseyiaspora punctispinosa*, the consistent occurrence of *Podosporites amicus* and the increased diversity of *Triadispora* spp. (Fig. 4a).

Biozonal assemblages: The zone is characterized by diverse assemblages with common specimens of *Angustisulcites* spp., *Aratrisporites* spp., *Illinites chitonoides*, *Striatoabieites* spp. and *Triadispora* spp. (Vigran *et al.* 2014, p. 71).

Occurrence: The zone has been recorded in the Botneheia Formation (Muen Member) from sections on Svalbard (Vigran *et al.* 2014). In the Barents Sea, the zone is recognized in stratigraphical cores and exploration wells penetrating the Steinkobbe and Kobbe formations on the Svalis Dome and Sentralbanken High, and in the Hammerfest, Maud and Nordkapp basins (Vigran *et al.* 2014; Paterson & Mangerud, 2017).

Biostratigraphic correlation: The *Triadispora obscura* Zone correlates with the *Aratrisporites macrocavatus* – *Triadispora plicata* – *Jerseyiaspora punctispinosa* – *Kraeuselisporites apiculatus* Concurrent Range Zone ('Svalis-6') of Vigran *et al.* (1998). The zone is also equivalent to the lower part of 'Assemblage K' of Hochuli *et al.* (1989), and partially equivalent to 'Floral Phase 4' of Hochuli & Vigran (2010). In the Russian Barents Sea, the last occurrence *Densoisporites nejburgii* occurs in the 'T_2a palynocomplex' (Mørk *et al.* 1993), the upper part of which likely correlates with the *Triadispora obscura* Zone (Fig. 3).

Age: The zone is dated as middle Anisian by a rich ammonoid fauna belonging to the *Anagymnotoceras varium* Zone which was recorded in Svalis Dome core 7323/07-U-01 (Vigran *et al.* 1998, 2014, p. 71).

3.a.3. Protodiploxypinus decus Zone

Definition: Vigran *et al.* (2014, p. 71) defines the base of the *Protodiploxypinus decus* Zone on the first common occurrence of *Chasmatosporites* spp. and *Illinites chitonoides* (Fig. 4a). Other taxa with first occurrences include *Camarozonosporites rudis* and *Retisulcites perforatus*. According to range data presented by Vigran *et al.* (2014), the upper limit of the zone is defined

https://doi.org/10.1017/S0016756819000906 Published online by Cambridge University Press

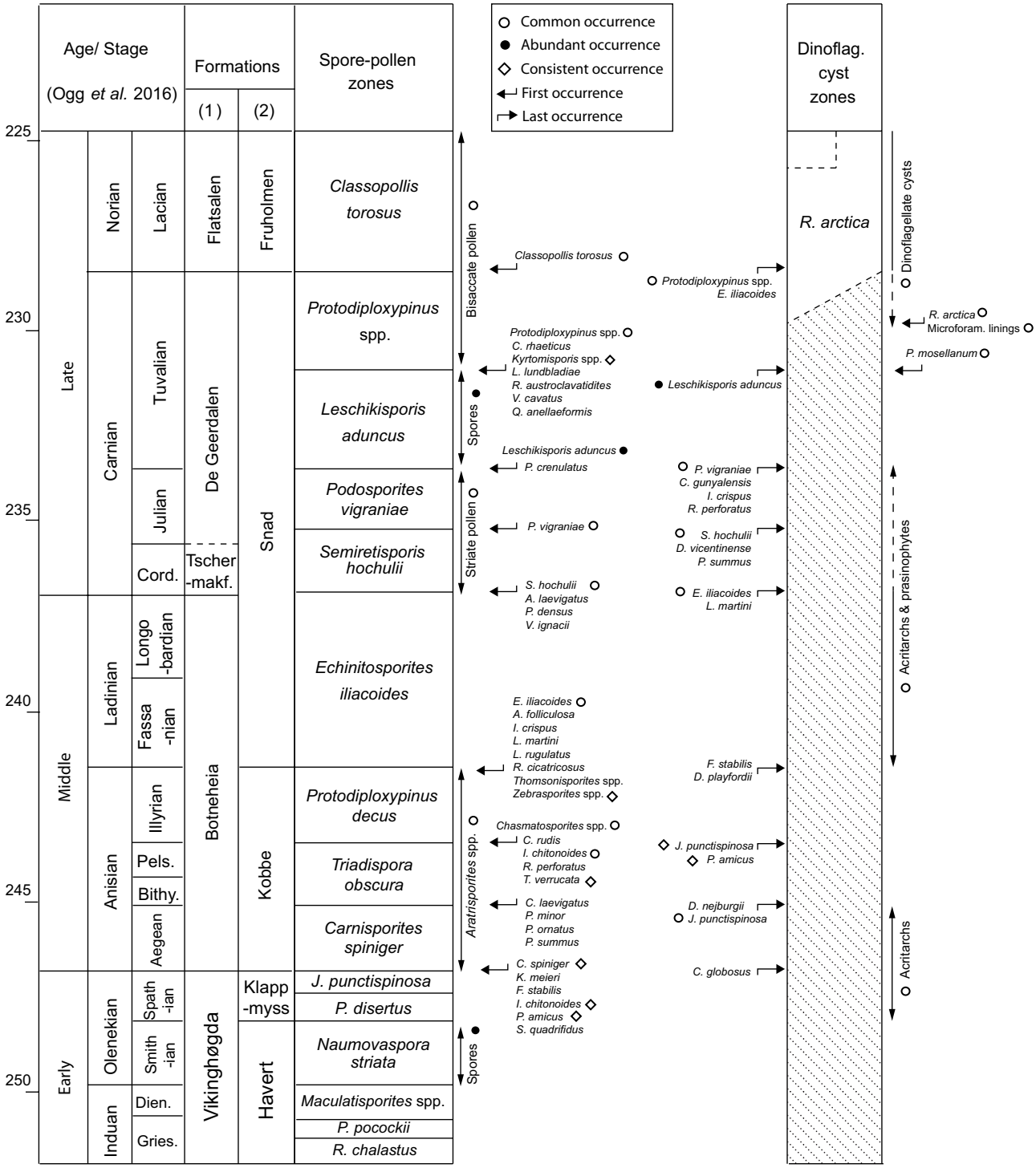

Fig. 4. (a) Anisian–Norian and (b) Norian–Rhaetian biozonal events. Formations from (1) eastern Svalbard and (2) Norwegian Barents Shelf. Timescale after Ogg *et al.* (2016).

https://doi.org/10.1017/S0016756819000906 Published online by Cambridge University Press

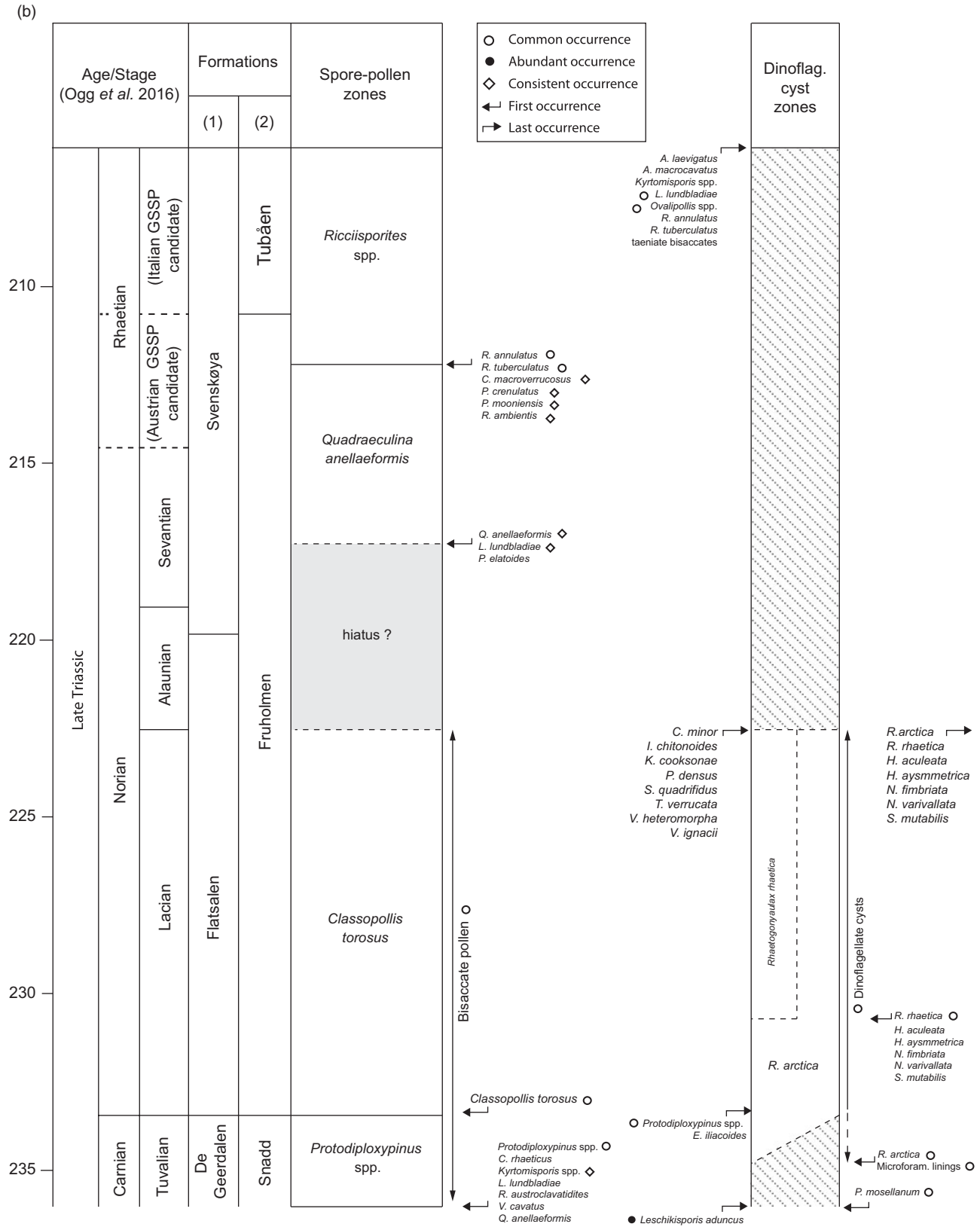

Fig. 4. (Continued)

https://doi.org/10.1017/S0016756819000906 Published online by Cambridge University Press

Table 1. Definition of the biostratigraphic event terms

Biostratigraphic event name	Definition
First occurrence (FO)	First regional occurrence of a taxon; may coincide with FCO
First consistent occurrence (FCO)	Taxon present in the majority of overlying samples, but sporadic or absent below; may coincide with FO
Common occurrence	Abundance of taxon > 10% of the total assemblage
Abundant occurrence	Abundance of taxon > 30% of the total assemblage
Last occurrence (LO)	Last regional occurrence of a taxon; may coincide with LCO
Last consistent occurrence (LCO)	Taxon present in the majority of underlying samples, but sporadic or absent above; may coincide with LO
Sporadic occurrence	Taxon intermittently present within its range
Rare occurrence	Taxon comprises < 1% of the total assemblage

by the last occurrences of *Densoisporites playfordii*, *Falcisporites stabilis*, *Kraeuselisporites apiculatus*, *Jerseyiaspora punctispinosa*, *Protodiploxypinus decus* and *P. ornatus*.

Biozonal assemblages: The zone is characterized by abundant striate pollen, including *Striatoabieites* spp. and *Lunatisporites* spp., together with non-striate pollen such as *Illinites chitonoides* (Vigran *et al.* 2014, p. 71). *Aratrisporites* spp. remains a common to abundant element of the zone. Marine palynomorphs are also relatively common, as is the fresh- to brackish-water alga *Plaesiodictyon mosellanum* (Vigran *et al.* 2014, p. 71).

Occurrence: The zone has been recorded in the Bravaisberget (Passhatten Member) and correlative Botneheia (Muen Member) formations on Svalbard (Vigran *et al.* 2014). It is also observed in core material from the Steinkobbe Formation on the Svalis Dome, and in the upper Klappmyss and Kobbe formations in the Hammerfest, Maud and Nordkapp basins and on the Sentralbanken High (Vigran *et al.* 2014; Paterson & Mangerud, 2017).

Comments: While Vigran *et al.* (2014) defined the top of the zone by the last occurrence of *Kraeuselisporites apiculatus*, *Jerseyiaspora punctispinosa*, *Protodiploxypinus decus* and *P. ornatus*, subsequent studies by the current authors have observed these taxa to have considerably longer stratigraphic ranges (Paterson & Mangerud, 2017; Paterson *et al.* 2017, 2019*a*). However, the possibility that these taxa are reworked into younger deposits cannot be excluded.

Biostratigraphic correlation: The *Protodiploxypinus decus* Zone was defined by Vigran *et al.* (2014, p. 71) from the Steinkobbe Formation in Svalis Dome cores 7323/7-U-7 and 7323/7-U-9. The zone incorporates the *Protodiploxypinus decus* – *P. gracilis* – *Chasmatosporites* sp. A – *Kraeuselisporites apiculatus* Concurrent Range Zone ('Svalis-7' of Vigran *et al.* 1998). The *Protodiploxypinus decus* Zone is also correlative of 'floral phases 5–7' of Hochuli & Vigran (2010). The zone likely correlates with the 'T_2a–l palynocomplex' of the Russian Barents Sea (Fig. 3).

Age: The zone is dated as late Anisian based on an abundant ammonoid fauna comprising *Frechites* sp. and *Parapopanoceras* sp., recorded in Svalis Dome core 7323/07-U-09, and assigned to the *Frechites laqueatus* Zone (Vigran *et al.* 1998, 2014, p. 71). However, Rhenium–Osmium (Re-Os) geochronology from Svalbard and the Svalis Dome more broadly constrains the age as late Anisian – Ladinian (Xu *et al.* 2009).

3.b. Ladinian

3.b.1. Echinitosporites iliacoides Zone

Definition: The *Echinitosporites iliacoides* Zone was defined by Vigran *et al.* (2014, p. 72) based on the first occurrence of *Echinitosporites iliacoides*. According to our observations and range data presented by Vigran *et al.* (2014), other taxa with first occurrences at the base of the zone include *Annulispora folliculosa*, *Institisporites crispus*, *Lagenella martini*, *Lycopodiacidites rugulatus*, *Rogalskaisporites cicatricosus*, *Thomsonisporites toralis*, *T. undulatus*, *Zebrasporites laevigatus* and *Z. interscriptus*. The top of the zone is defined by the last common occurrence of *Echinitosporites iliacoides* and *Lagenella martini*.

Biozonal assemblages: The zone is characterized by a diverse taxonomic association dominated by bisaccate pollen, including the common occurrence of non-taeniate pollen (Vigran *et al.* 2014, p. 72). The zone also contains abundant and diverse *Aratrisporites* spp.

Occurrence: On Svalbard, the *Echinitosporites iliacoides* Zone has been recorded in samples from the Bravaisberget Formation (Somovbreen and Van Keulenfjorden members) and the correlative upper Muen – Blanknuten members of the Botneheia Formation equivalent (Vigran *et al.* 2014). In the Barents Sea, the zone is recorded in the subsurface Botneheia Formation east of Kong Karls Land, in the upper Kobbe Formation on the Bjarmeland Platform, Loppa High and Nordkapp Basin, and in the lower Snadd Formation on the Loppa High and in the Maud Basin (Vigran *et al.* 2014; Paterson & Mangerud 2017).

Comments: According to Vigran *et al.* (2014, p. 72) the taxa *Staurosaccites quadrifidus* and *Triadispora verrucata* have their first occurrences in the lower part of the zone. However, the present authors have observed rare occurrences beginning in the lower Anisian Kobbe Formation in the Nordkapp Basin (Paterson & Mangerud 2017; Rossi *et al.* 2019). Despite being a marker for the base of the zone, the taxon *A. astigmosus* has only ever been observed to be a sporadic element among our Carnian assemblages. This issue was highlighted in Paterson *et al.* (2017), who suggested that the taxon *Podosporites* cf. *amicus* (now *P. vigraniae* sp. nov.) may have been misidentified as *A. astigmosus* by previous authors, leading to an overestimation of *A. astigmosus* in the Carnian strata of the Barents Sea region. This speculation was based on the similarity between the specimen of *A. astigmosus* illustrated by Klaus (1960, pl. 28, 2) and specimens of *P. vigraniae* with weakly developed sacci observed in our material. Since this matter remains unresolved, in this paper we define the top of the *Echinitosporites iliacoides* Zone by the base of the *Semiretisporis hochulii* Zone, which is the oldest of our subdivisions of the former *Aulisporites astigmosus* Zone.

Biostratigraphic correlation: The *Echinitosporites iliacoides* Zone correlates with assemblages 'H and I' of Hochuli *et al.* (1989), and incorporates the *Ovalipollis pseudoalatus* – *Echinitosporites iliacoides* – *Cordaitina gunyalensis* Concurrent Range Zone of Vigran *et al.* (1998). The zone likely corresponds, at least in part, to the 'T_2l palynocomplex' of the Russian Barents Sea. However, in contrast

https://doi.org/10.1017/S0016756819000906 Published online by Cambridge University Press

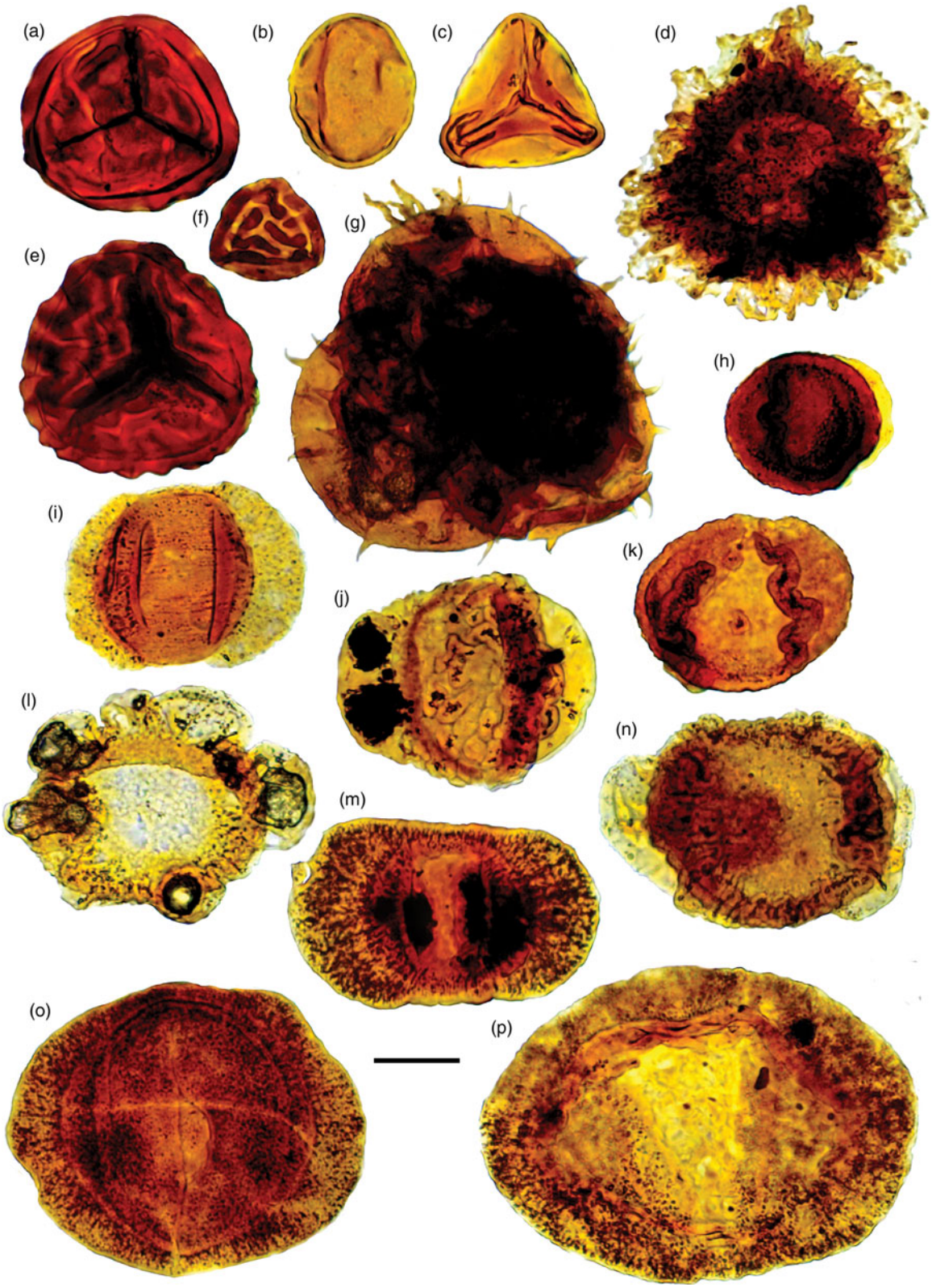

Fig. 5. Palynomorph taxa from the Late Triassic (early Carnian) *Semiretisporis hochulii* Zone. Palaeontological Museum Oslo (PMO) number followed by England Finder Coordinates. Scale bars = 20 μm. (a) *Camarozonosporites rudis*, PMO 234.369 B, R48-4; (b) *Leschikisporis aduncus*, PMO 234.372 D, R40; (c) *Dictyophyllidites mortonii*, PMO 234.374 A, G52; (d) *Semiretisporis hochulii* sp. nov., holotype, PMO 234.369 A, K54; (e) *Lycopodiacidites rugulatus*, PMO 234.373 A, U52-4; (f) *Striatella parva*, PMO 234.373 C, X49; (g) *Kraeuselisporites* sp. tetrad, PMO 234.375 A, G52-1; (h) *Podosporites amicus*, PMO 234.373 B, N39-3; (i) *Striatoabieites balmei*, PMO 234.372 A, K45-1; (j) *Triadispora verrucata*, PMO 234.370 B, T45-3; (k) *Podosporites vigraniae* sp. nov., holotype, PMO 234.374 B, S42-2; (l) *Dyupetalum vicentinense*, PMO 234.371 C, M49-1; (m) *Voltziaceaesporites heteromorpha*, PMO 234.371 A, H46-2; (n) *Institisporites crispus*, PMO 234.371 B, M44-1; (o) *Staurosaccites quadrifidus*, PMO 234.372 C, Q47-4; and (p) *Illinites chitonoides*, PMO 234.370 A, S45-3.

https://doi.org/10.1017/S0016756819000906 Published online by Cambridge University Press

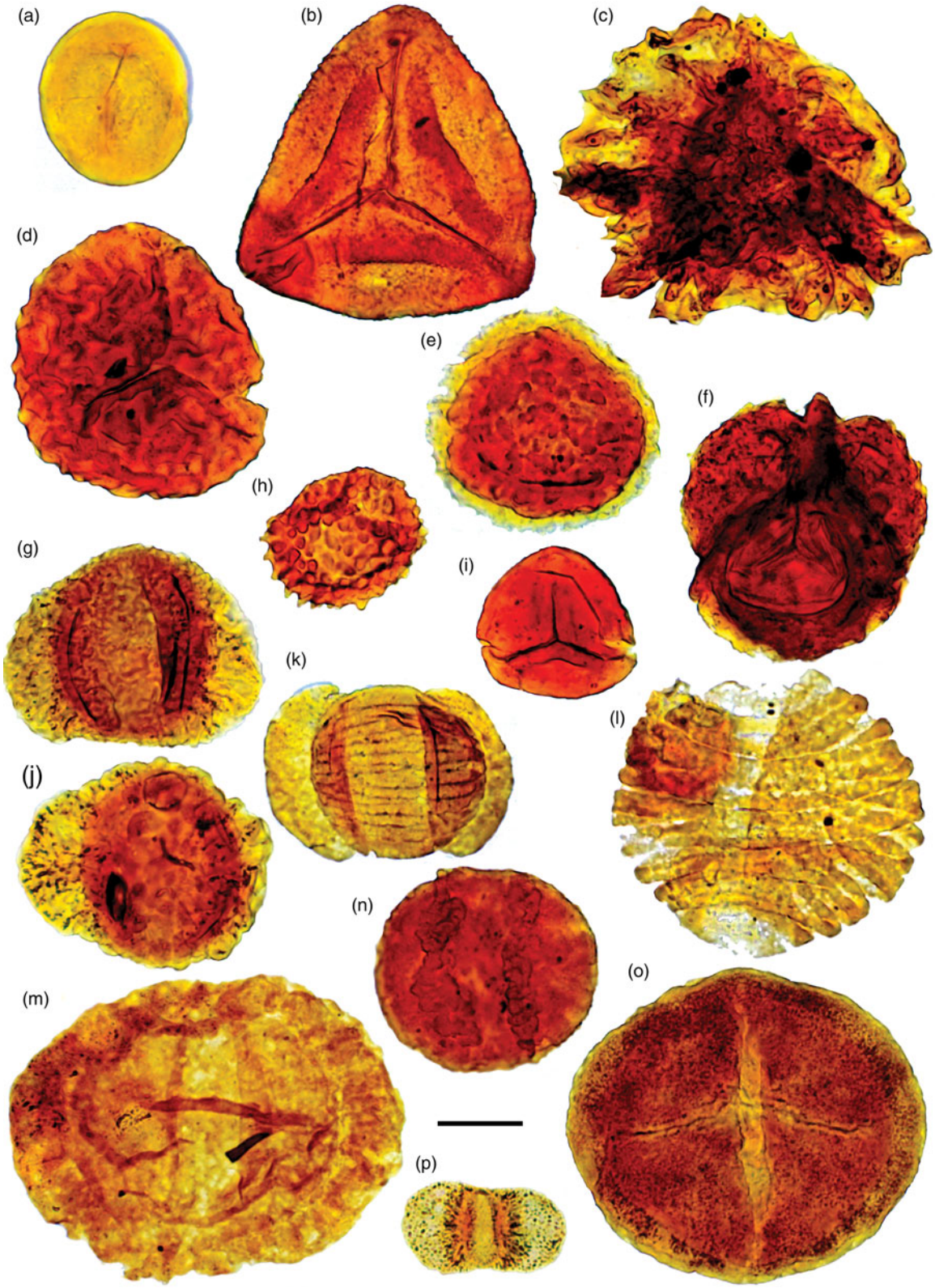

Fig. 6. Palynomorph taxa from the Late Triassic (early Carnian) *Podosporites vigraniae* Zone. Palaeontological Museum Oslo (PMO) number followed by England Finder Coordinates. Scale bars = 20µm. (a) *Leschikisporis aduncus*, PMO 234.381 A, H56; (b) *Kyrtomisporis moerki* sp. nov., holotype, PMO 234.376 B, M44-1; (c) *Kraeuselisporites* ? *dentatus*, PMO 234.378 B, N45; (d) *Lycopodiacidites rugulatus*, PMO 234.380 B, G54-2; (e) *Kraeuselisporites cooksonae*, PMO 234.380 A, E54; (f) *Kraeuselisporites cooksonae* tetrad, PMO 234.378 A, D56-1; (g) *Triadispora plicata*, PMO 234.383 F, J56-3; (h) *Carnisporites spiniger*, PMO 234.383 D, E55-3; (i) *Camarozonosporites laevigatus*, PMO 234.384 A, J45-2; (j) *Triadispora verrucata*, PMO 234.380 C, G49-4; (k) *Striatoabieites balmei*, PMO 234.383 B, C51-2; (l) *Schizaeoisporites worsleyi*, PMO 234.383 C, D51-2; (m) *Illinites chitonoides*, PMO 234.377 A, R54-4; (n) *Podosporites vigraniae* sp. nov., PMO 234.379 A, G47-1; (o) *Staurosaccites quadrifidus*, PMO 234.383 A, C48-2; and (p) *Vitreisporites pallidus*, PMO 234.382 A, J45-1.

https://doi.org/10.1017/S0016756819000906 Published online by Cambridge University Press

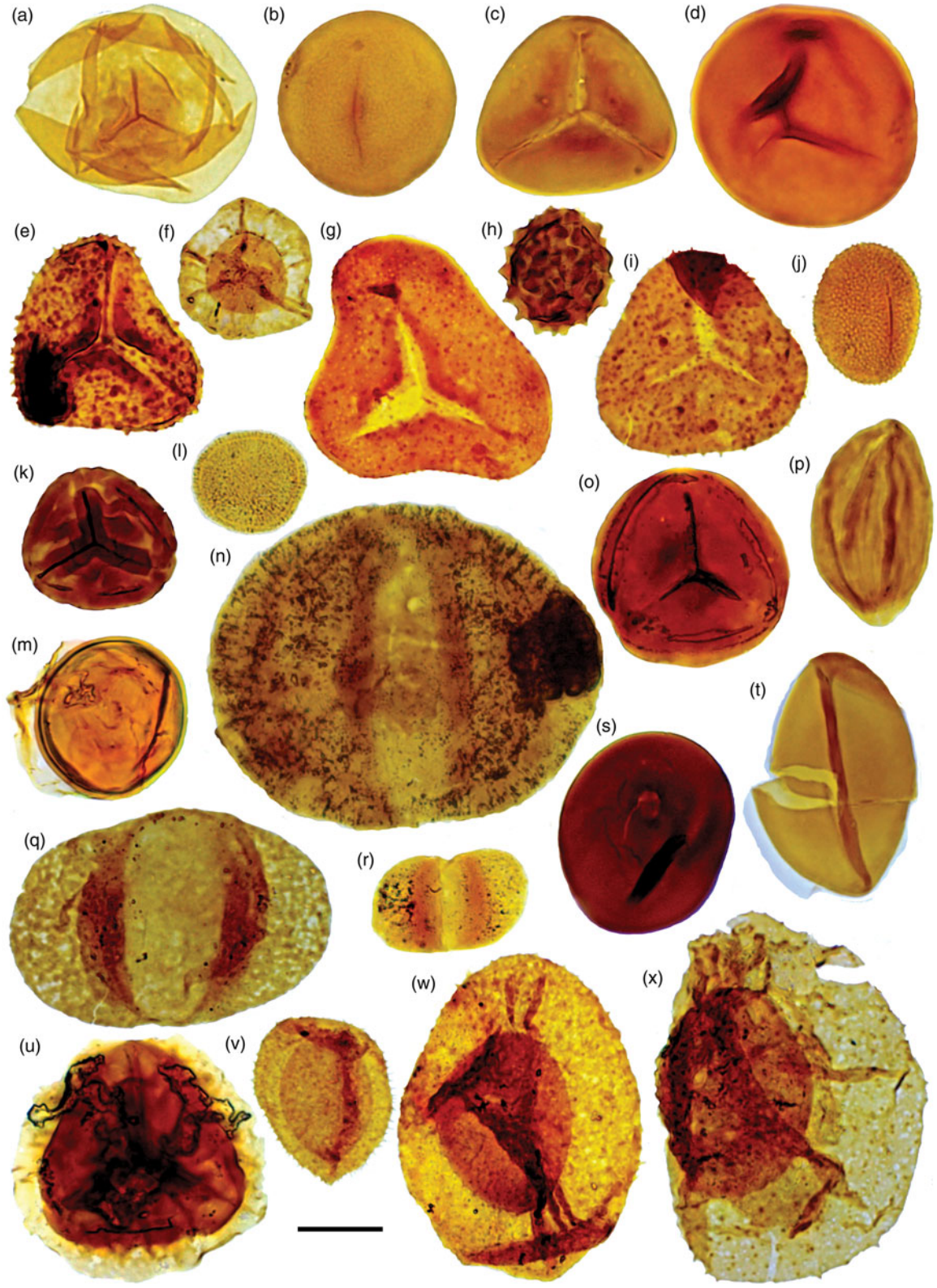

Fig. 7. Palynomorph taxa from the Late Triassic (late Carnian) *Leschikisporis aduncus* Zones. Palaeontological Museum Oslo (PMO) number followed by England Finder Coordinates. Scale bars = 20μm. (a) *Calamospora tener*, PMO 234.391 A, C44-4; (b) *Leschikisporis aduncus*, PMO 234.391 D, J44-4; (c) *Deltoidospora* sp., PMO 234.391 B, C47; (d) *Punctatisporites fungosus*, PMO 234.387 D, W59; (e) *Clathroidites papulosus*, PMO 234.387 A, K40; (f) *Thomsonisporites toralis*, PMO 234.394 A, N64; (g) *Concavisporites scabratus*, PMO 234.387 C, U54-4; (h) *Anapiculatisporites lativerrucosus*, PMO 234.392 C, H60-4; (i) *Conbaculatisporites hopensis*, PMO 234.388 A, M50-1; (j) *Apiculatisporis parvispinosus*, PMO 234.391 C, C55-2; (k) *Camarozonosporites rudis*, PMO 234.392 D, J44-2; (l) *Vallasporites ignacii*, PMO 234.391 E, K41; (m) *Cymatiosphaera* sp. 1 *sensu* Hochuli *et al.* (1989), PMO 234.390 A, K45-1; (n) *Illinites chitonoides*, PMO 234.392 F, M61-1; (o) *Camarozonosporites laevigatus*, PMO 234.393 A, D61-4; (p) *Ephedripites steevesii*, PMO 234.392 B, G61; (q) *Alisporites* sp., PMO 234.387 B, T44; (r) *Vitreisporites pallidus*, PMO 234.394 B, O65; (s) *Aulisporites canalis*, PMO 234.389 B, E39-4; (t) *Aratrisporites laevigatus*, PMO 234.395 A, U50-4; (u) *Zebrasporites kahleri*, PMO 234.393 B, Y64-1; (v) *Aratrisporites scabratus*, PMO 234.387 E, X49-3; (w) *Aratrisporites macrocavatus*, PMO 234.389 A, D52; and (x) *Aratrisporites fischeri*, PMO 234.392 A, F47-4.

https://doi.org/10.1017/S0016756819000906 Published online by Cambridge University Press

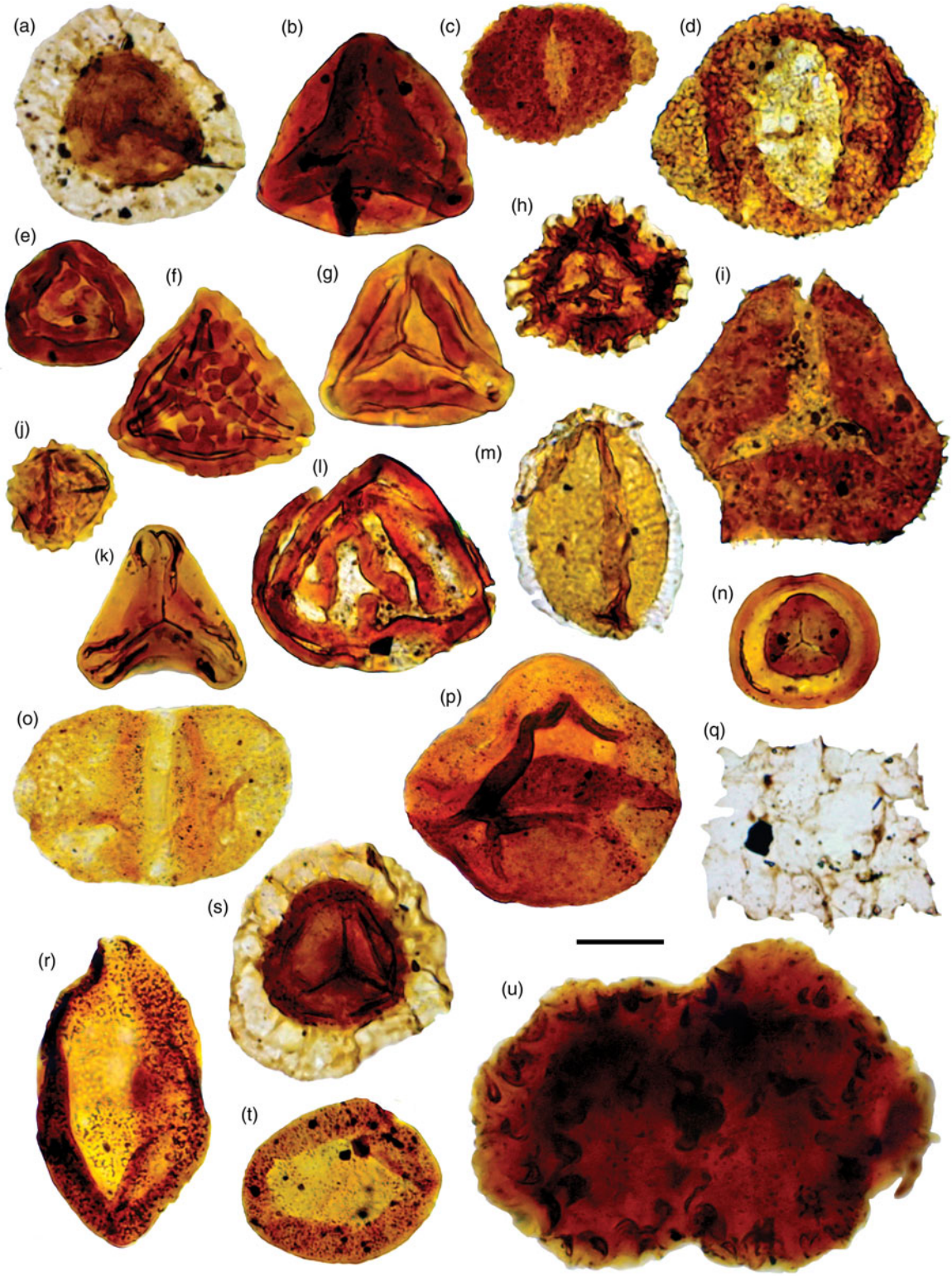

Fig. 8. Palynomorph taxa from the Late Triassic (late Carnian) *Protodiploxypinus* spp. Zone. Palaeontological Museum Oslo (PMO) number followed by England Finder Coordinates. Scale bars = 20µm. (a) *Velosporites cavatus*, PMO 234.399 A, M37-2; (b) *Kyrtomisporis laevigatus*, PMO 234.403 A, X32; (c) *Protodiploxypinus minor*, PMO 234.398 C, O58; (d) *Protodiploxypinus decus*, PMO 234.405 A, D58-1; (e) *Striatella parva*, PMO 234.403 B, P31-4; (f) *Kyrtomisporis speciosus*, PMO 234.401 C, T33-4; (g) *Concavisporites crassexinus*, PMO 234.405 F, S60; (h) *Retitriletes austroclavatidites*, PMO 234.405 C, H40-4; (i) *Concavisporites hopensis*, PMO 234.405 B, H38-4; (j) *Anapiculatisporites lativerrucosus*, PMO 234.399 B, M44; (k) *Dictyophyllidites mortonii*, PMO 234.401 D, W33-4; (l) *Striatella seebergensis* PMO 234.405 D, N32-2; (m) *Aratrisporites laevigatus*, PMO 234.405 E, N55-3; (n) *Annulispora folliculosa*, PMO 234.400 A, C34-2; (o) *Alisporites* sp., PMO 234.398 D, Y56-1; (p) *Araucariacites australis*, PMO 234.398 E, Y50; (q) *Plaesiodictyon mosellanum*, PMO 234.402 A, O56-2; (r) *Chasmatosporites hians*, PMO 234.398 B, H36-1; (s) *Cingulizonates rhaeticus*, PMO 234.401 A, S29-3; (t) *Chasmatosporites apertus*, PMO 234.398 A, G47-4; and (u) *Botryococcus* sp., PMO 234.401 B, T30-1.

https://doi.org/10.1017/S0016756819000906 Published online by Cambridge University Press

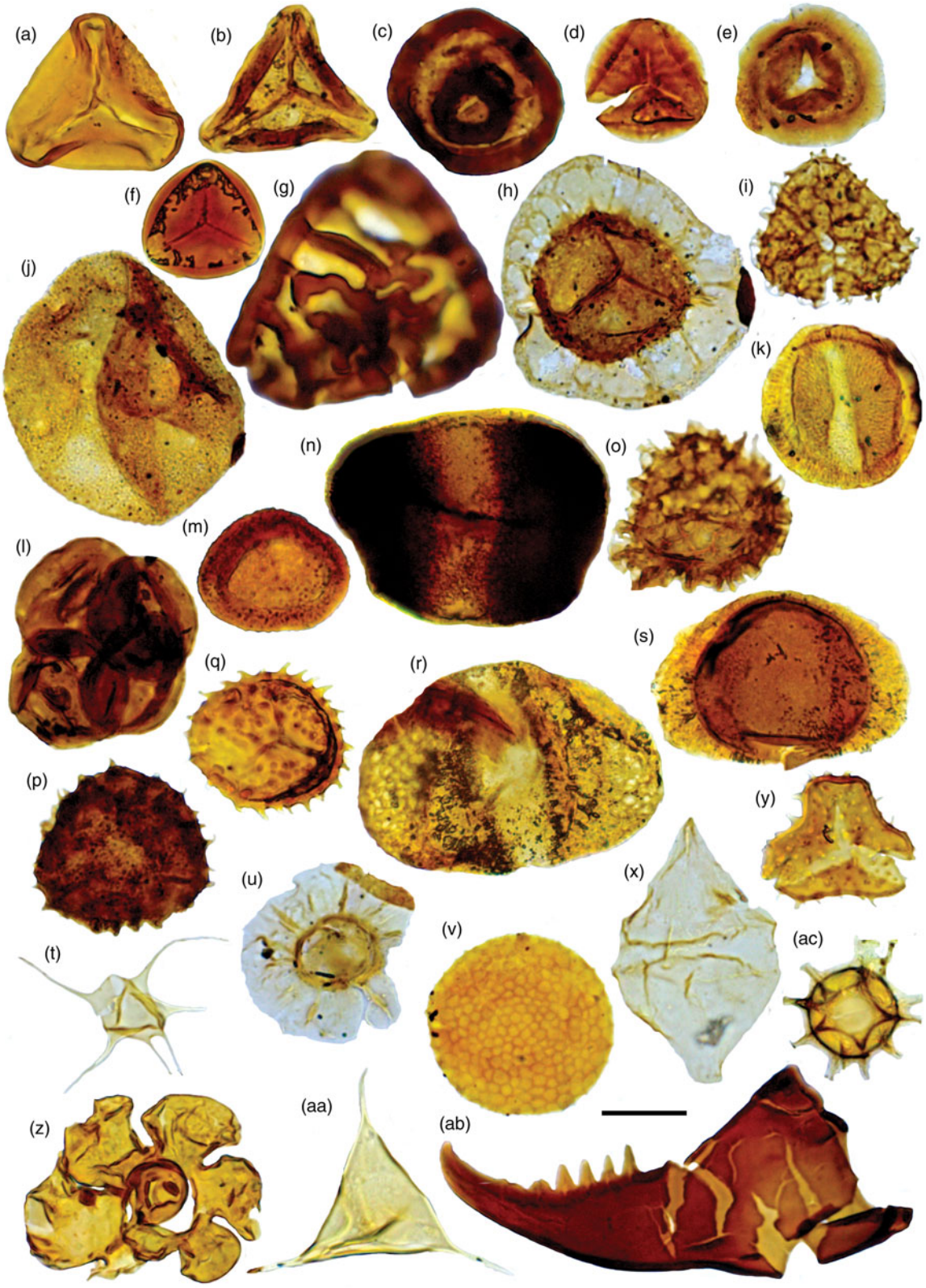

Fig. 9. Palynomorph taxa from the Late Triassic (latest Carnian – early Norian) *Classopollis torosus*, *Rhaetogonyaulax arctica* and *R. rhaetica* zones. Palaeontological Museum Oslo (PMO) number followed by England Finder Coordinates. Scale bars = 20µm. (a) *Dictyophyllidites mortonii*, PMO 234.410 B, D45-4; (b) *Concavisporites crassexinus*, PMO 234.386 D, S36-4; (c) *Annulispora folliculosa*, PMO 234.404 A, Q59-1; (d) *Zebrasporites interscriptus*, PMO 234.414 A, C41-4; (e) *Polycingulatisporites bicollateralis*, PMO 234.414 E, O50; (f) *Camarozonosporites laevigatus*, PMO 234.413 A, Y55; (g) *Kyrtomisporis speciosus*, PMO 234.412 A, K53; (h) *Velosporites cavatus*, PMO 234.414 F, O32-2; (i) *Retitriletes semimuris*, PMO 234.414 B, C54; (j) *Araucariacites australis*, PMO 234.414 C, K33; (k) *Quadraeculina anellaeformis*, PMO 234.411 E, N42-1; (l) *Classopollis torosus* tetrad, PMO 234.386 C, N47-2; (m) *Classopollis torosus*, PMO 234.386 A, D34-3; (n) *Vesicaspora fuscus*, PMO 234.410 C, F36-3; (o) *Retitriletes austroclavatidites*, PMO 234.386 E, S39; (p) *Kraeuselisporites reissingerii*, PMO 234.386 B, K55-2; (q) *Carnisporites spiniger*, PMO 234.410 E, G51-3; (r) *Alisporites* sp., PMO 234.410 D, F37-4; (s) *Triadispora boelchii*, PMO 234.410 F, M50; (t) *Baltisphaeridium* sp., PMO 234.411 D, J49-4; (u) *Pterospermella* sp., PMO 234.414 D, L33; (v) *Crassosphaera* sp., PMO 234.410 G, O37-1; (x) *Rhaetogonyaulax rhaetica*, PMO 234.411 F, R58-2; (y) *Lophotriletes novicus*, PMO 234.411 B, C42; (z) microforaminiferal test-lining, PMO 234.410 A, B46-4; (aa) *Veryhachium* sp., PMO 234.411 A, C34; (ab) scolecodont gen. et. sp. indet., PMO 234.411 C, E60-4; and (ac) ?*Cymatiosphaera* sp., PMO 234.412 B, L53-2.

https://doi.org/10.1017/S0016756819000906 Published online by Cambridge University Press

Fig. 10. Palynomorph taxa from the Late Triassic (Norian–Rhaetian) *Quadraeculina anellaeformis* and *Ricciisporites* spp. zones. Palaeontological Museum Oslo (PMO) number followed by England Finder Coordinates. Slides from well 7228/7-1A belong to Applied Petroleum Technology, Oslo. Scale bars = 20μm. (a) *Ricciisporites tuberculatus*, well 7228/7-1A 1506 m, F49-3; (b) *Cibotiumspora jurienensis*, well 7228/7-1A 1548 m, E44-2; (c) *Rogalskaisporites ambientis*, PMO 234.408 E, X52; (d) *Quadraeculina anellaeformis*, well 7228/7-1A 1506 m, W50-4; (e) *Polycingulatisporites mooniensis*, well 7228/7-1A 1506 m, B44-3; (f) ?*Tripartites* sp., well 7228/7-1A 1506 m, L48-4; (g) *Cerebropollenites macroverrucosus*, PMO 234.397 A, U37-2; (h) *Ricciisporites annulatus*, PMO 234.408 B, G35; (i) *Semiretisporis gothae*, well 7228/7-1A 1506 m, H29-1; (j) *Chasmatosporites hians*, PMO 234.396 A, K40-2; (k) *Lycopodiacidites rugulatus*, well 7228/7-1A 1506 m, R51-1; (l) *Retitriletes austroclavatidites*, PMO 234.408, G54-3; (m) *Cingulizonates rhaeticus*, PMO 234.409 A, G30-1; (n) *Zebrasporites laevigatus*, PMO 234.408 A, C39; (o) *Kyrtomisporis laevigatus*, PMO 234.408 D, O33-1; (p) *Chasmatosporites apertus*, well 7228/7-1A 1548 m, W37; (q) *Perinopollenites elatoides*, PMO 234.406 A, G35-3; (r) *Araucariacites australis*, well 7228/7-1A 1542 m, O34-3; (s) *Limbosporites lundbladiae*, well 7228/7-1A 1548 m, S51; and (t) *Kyrtomisporis gracilis*, PMO 234.407 A, X58-1.

https://doi.org/10.1017/S0016756819000906 Published online by Cambridge University Press

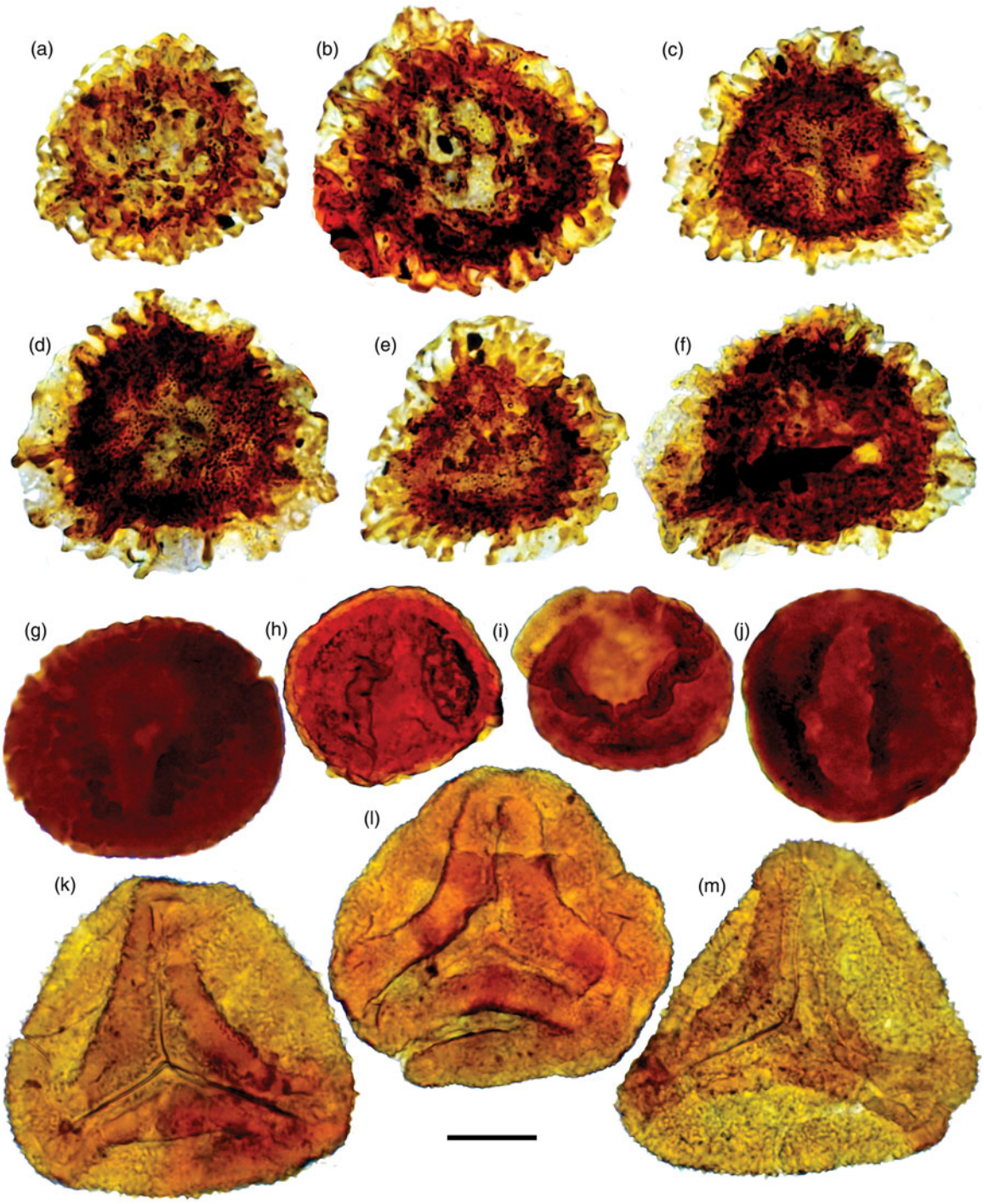

Fig. 11. Paratype specimens of new taxa described here. Palaeontological Museum Oslo (PMO) number followed by England Finder Coordinates. Scale bars = 20μm. (a–f) *Semiretisporis hochulii* sp. nov.: (a) PMO 234.367 A, C45-4; (b) PMO 234.367 B, K61; (c) PMO 234.372 E, U41-4; (d) PMO 234.368 B, G45; (e) PMO 234.368 A, F46-4; and (f) PMO 234.367 C, O49. (g–j) *Podosporites vigraniae* sp. nov.: (g) PMO 234.394 C, D49-2; (h) PMO 234.383 E, F44-1; (i) PMO 234.372 B, E37-4; and (j) PMO 234.392 E, L61-4. (k–m) *Kyrtomisporis moerki* sp. nov.: (k) PMO 234.385 A, V53-1; (l) PMO 234.376 C, Q40-1; and (m) PMO 234.376 A, K40-4.

to the Norwegian Barents Shelf, the highest abundance of *Echinitosporites iliacoides* there is recorded in the slightly younger 'T_2–T_3 palynocomplex' (Fefilova, 1988; Mørk *et al.* 1993).

Age: The *Echinitosporites iliacoides* Zone is dated as Ladinian based on the sparse occurrence of bivalves assigned to *Aparimella* spp. (Vigran *et al.* 1998, p. 118).

3.c. Carnian

3.c.1. Semiretisporis hochulii Zone

Definition: The *Semiretisporis hochulii* Zone was first described from the lowermost Snadd Formation in the Nordkapp Basin (Paterson & Mangerud 2017) and from the Tschermakfjellet Formation in the Sentralbanken area (Paterson *et al.* 2019*a*).

https://doi.org/10.1017/S0016756819000906 Published online by Cambridge University Press

The base of the zone is defined by the first common occurrence of *Semiretisporis hochulii* sp. nov., and the first occurrences of *Aratrisporites laevigatus*, *Patinasporites densus* and *Vallasporites ignacii* (Fig. 4a). The top of the zone is marked by the last common occurrences of *Dyupetalum vicentinense*, *Patinasporites summus* and *S. hochulii* sp. nov.

Biozonal assemblages: Characteristic taxa include *Aratrisporites fischeri*, *Araucariacites australis*, *Calamospora tener*, *Conbaculatisporites* spp., *Deltoidospora* spp., *Echinitosporites iliacoides* (rare/sporadic), *Illinites chitonoides*, *Leschikisporis aduncus*, *Podosporites vigraniae* sp. nov., *Semiretisporis hochulii* sp. nov., *Striatella seebergensis*, *Striatoabieites balmei*, *S. multistriatus* and *Triadispora verrucata*. A representative association of species present in the zone are illustrated in Figure 5.

Occurrence: The *Semiretisporis* Zone was first recorded informally as 'assemblage SBS-VII' from the basal Snadd Formation in Nordkapp Basin wells 7228/2-1s and 7228/9-1s (Paterson & Mangerud 2017). Comparable assemblages were subsequently recorded as 'assemblage SBH-I' in preparations from the 'Tschermakfjellet' and Snadd formations in shallow stratigraphical cores 7533/3-U-7 and 7534/4-U-1 from the Sentralbanken High area (Paterson *et al.* 2019*a*). The zone is given formal status here.

Biostratigraphic correlation: The *Semiretisporis hochulii* Zone is likely equivalent to 'Assemblage G' of Hochuli *et al.* (1989, p. 143) and the lowermost part of the *Aulisporites astigmosus* Zone of Vigran *et al.* (2014, p. 73) (Fig. 3). The common occurrence of *Semiretisporis* is a feature noted in the lower De Geerdalen Formation on central Spitsbergen by Mueller *et al.* (2016). The *Semiretisporis hochulii* Zone likely corresponds to the low-productivity assemblages with consistent *Semiretisporis* '*barentsi*' (=*S. hochulii* sp. nov.) tentatively assigned by van Veen (1985) to his informal 'palynozone VIII' from well 7120/9-2. At the time, van Veen (1985) noted that the assemblages were restricted to this one well; however, recovery of comparable assemblages on Spitsbergen (Mueller *et al.* 2016) and elsewhere in the Barents Sea (Paterson & Mangerud 2017; Paterson *et al.* 2019*a*) suggests it has a regional distribution.

The *Semiretisporis hochulii* Zone likely corresponds to the transitional 'T_2–T_3 palynocomplex' of the Russian Barents Sea (Fig. 3) based on its relative stratigraphic position and the composition of over- and underlying zones. However, as noted by Mørk *et al.* (1993) the latter zone contains abundant *Echinitosporites iliacoides*, which is comparatively rare in age-equivalent assemblages in the Norwegian Arctic. This disparity may be the result of reworking, or due to the parent plant taxon possibly having a longer range in the more proximal areas to the east.

Age: The *Semiretisporis hochulii* Zone is dated as earliest Carnian (Julian) based on the last consistent occurrence of *Echinitosporites iliacoides*, which on Bjørnøya (Mørk *et al.* 1990) occurs in strata containing the ammonoid *Daxatina* cf. *canadensis* (e.g. Vigran *et al.* 2014, p. 72–73). Re-Os geochronology of the underlying *Echinitosporites iliacoides* Zone in core material from offshore Kong Karls Land (Xu *et al.* 2014) provides an age of 236.6 ± 0.4 Ma, which dates the base of *Semiretisporis hochulii* Zone as early Carnian.

3.c.2. Podosporites vigraniae Zone

Definition: The *Podosporites vigraniae* Zone was originally described as the '*Podosporites* cf. *amicus* Assemblage' from the Snadd Formation in the Kong Karls Land area by Paterson *et al.* (2016). It is elevated to full zonal status here. The zone is characterized by a diverse taxonomic association containing common to abundant specimens of *Podosporites vigraniae* sp. nov., without common *Semiretisporis hochulii* sp. nov. or dominant *Leschikisporis aduncus*, which typify assemblages from the underlying and overlying zones, respectively (Fig. 4a). The top of the zone is defined by the last common occurrence of *P. vigraniae*, the last occurrences of *Cordaitina gunyalensis*, *Institisporites crispus* and *Retisulcites perforatus*, and the first occurrence of dominant *Leschikisporis aduncus*, marking the base of the *Leschikisporis aduncus* Zone.

Biozonal assemblages: The zone contains a highly diverse palynological assemblage characterized by an association of fern, bryophyte, lycopsid and sphenopsid spores, together with conifer, cycad-ginkgophyte and pteridosperm pollen. A representative selection of species present in the zone is illustrated in Figure 6. Spore taxa recorded include *Annulispora folliculosa*, *Aratrisporites laevigatus*, *A. paenulatus*, *Calamospora tener*, *Camarozonosporites rudis*, *Carnisporites spiniger*, *Conbaculatisporites* spp., *Deltoidospora* spp., *Densosporites fissus*, *Dictyophyllidites mortonii*, *Kraeuselisporites cooksonae*, *Kyrtomisporis moerki* sp. nov., *Leschikisporis aduncus*, *Limatulasporites limatulus*, *Lycopodiacidites rugulatus*, *Lycopodiumsporites semimuris*, *Neoraistrickia* spp., *Reticulatisporites* sp., *Semiretisporis hochulii* sp. nov. (sporadic), *Striatella parva*, *S. seebergensis*, *Thomsonisporites toralis*, *Tigrisporites halleinis* and *Zebrasporites* spp.

Pollen taxa present in the assemblage include *Alisporites* spp., *Angustisulcites klausii*, *Araucariacites australis*, *Aulisporites astigmosus*, *Brachysaccus* spp., *Camerosporites secatus*, *Chasmatosporites* spp., *Chordasporites singulichorda*, *Dyupetalum vicentinense*, *Enzonalasporites vigens*, *Eucommiidites intrareticulatus*, *Illinites chitonoides*, *Infernopollenites* sp., *Institisporites crispus*, *Kuglerina meieri*, *Lunatisporites acutus*, *L. noviaulensis*, *Ovalipollis ovalis*, *Partitisporites* sp., *Patinasporites densus*, *Podosporites amicus*, *P. vigraniae* sp. nov., *Protodiploxypinus* spp., *Pseudoenzonalasporites summus*, *Pseudoquadrisaccus irregularis*, *Retisulcites* spp., *Schizaeoisporites worsleyi*, *Striatoabieites* spp., *Staurosaccites quadrifidus*, *Triadispora* spp. and *Vitreisporites pallidus*.

Occurrence: The *Podosporites vigraniae* Zone has been observed in the 'Tschermakfjellet' and Snadd formations from offshore Kong Karls Land (Paterson *et al.* 2017). The zone has also been recorded in the Snadd Formation in Hammerfest Basin well 7120/12-2 (2425–2645 m), and in Nordkapp Basin wells 7228/2-1s (1911–2215 m) and 7228/9-1s (1373.5–1557 m) (Paterson & Mangerud 2017).

Biostratigraphic correlation: The *Podosporites vigraniae* Zone correlates with 'Assemblage F' of Hochuli *et al.* (1989) and the lower part of the *Aulisporites astigmosus* Zone of Vigran *et al.* (2014). The zone probably corresponds to the undifferentiated Carnian 'T_2k palynocomplex' of the Russian Barents Sea, which also contains abundant *Leschikisporis aduncus* and *Podosporites amicus* (Mørk *et al.* 1993; Fefilova, 2013) (Fig. 3).

Age: Re-Os geochronology of the underlying *Echinitosporites iliacoides* Zone in core material from offshore Kong Karls Land (Xu *et al.* 2014) provides an age of 236.6 ± 0.4 Ma, which constrains the ages of the *Semiretisporis hochulii* and *Podosporites vigraniae* zones as no older than early Carnian (Paterson *et al.* 2017). Furthermore, dating of the succeeding *Leschikisporis aduncus* Zone on Hopen indicates that the top of the *Podosporites vigraniae* is no younger than late Carnian (Tuvalian 2) (Lord *et al.* 2014; Paterson & Mangerud, 2015).

https://doi.org/10.1017/S0016756819000906 Published online by Cambridge University Press

3.c.3. Leschikisporis aduncus Zone

Definition: The *Leschikisporis aduncus* Zone was described as the '*Leschikisporis aduncus* Assemblage' in preparations from the lower exposures of the De Geerdalen Formation (= middle De Geerdalen Formation) on Hopen by Paterson & Mangerud (2015). It is elevated to full zonal status here. The base of the zone is defined by the first occurrence of dominant *Leschikisporis aduncus*, typically in association with *Apiculatasporites hirsutus*, *A. lativerrucosus*, *Apiculatisporis parvispinosus*, *Calamospora tener* and *Clathroidites papulosus* (Fig. 4a). The zone is characterized by a low-diversity taxonomic association comprising mainly palynomorphs of hygrophytic affinity such as bryophyte, fern, lycopsid and sphenopsid spores (Fig. 7) (see Paterson *et al.* 2016, table 1: Paterson *et al.* 2017, table 4). The top of the zone is defined by the base of the overlying *Protodiploxypinus* spp. Zone and the last occurrence of dominant *L. aduncus*.

Biozonal assemblages: The zone is typified by an association of spore taxa including *Annulispora folliculosa*, *Apiculatasporites hirsutus*, *A. lativerrucosus*, *Apiculatisporis parvispinosus*, *Aratrisporites fischeri*, *A. granulatus*, *A. scabratus*, *Calamospora tener*, *Camarozonosporites rudis*, *Clathroidites papulosus*, *Conbaculatisporites hopensis*, *Deltoidospora* spp., *Dictyophyllidites mortonii*, *Kraeuselisporites cooksonae*, *Porcellispora longdonensis*, *Striatella parva*, *Zebrasporites interscriptus* and *Z. laevigatus*. Pollen grains comprise a relatively minor component of this assemblage: taxa include *Araucariacites australis*, *Aulisporites astigmosus*, *Chasmatosporites* spp., *Cycadopites* spp., *Eucommiidites* sp., *Illinites chitonoides*, *Ovalipollis ovalis*, *Steevesipollenites* sp., *Triadispora verrucata* and *Vesicaspora fuscus*.

Occurrence: The *Leschikisporis aduncus* Zone has been observed in preparations from the De Geerdalen (below the Hopen Member) on Hopen (Paterson & Mangerud, 2015), Spitsbergen (Rismyhr *et al.* 2018) and in shallow stratigraphical cores from the Sentralbanken High (Paterson *et al.* 2018). The zone has also been recorded in the middle part of the Snadd Formation in Hammerfest Basin 7228/2-1s (1766.5–1891 m) and 7228/9-1s (sample 1358 m) (Paterson & Mangerud 2017).

Biostratigraphic correlation: The *Leschikisporis aduncus* Zone corresponds to the informal 'middle' Carnian 'assemblages D and E' of Hochuli *et al.* (1989), 'Floral Phase 12' (Hochuli & Vigran, 2010, Fig. 2) and to the upper part of the *Aulisporites astigmosus* Zone of Vigran *et al.* (2014). On Hopen, the *L. aduncus* Zone correlates with an interval rich in lycopsid megaspores, recently defined as the *Dijkstraisporites beutleri* Zone (Paterson *et al.* 2019*b*). Together with the preceding *Podosporites vigraniae* Zone, the *Leschikisporis aduncus* Zone likely correlates with the undifferentiated Carnian 'T_2k palynocomplex' of the Russian Barents Sea (Mørk *et al.* 1993; Fefilova, 2013) (Fig. 3).

Age: The zone is dated as late Carnian (Tuvalian 2–3) based on magnetostratigraphy (Lord *et al.* 2014; Paterson & Mangerud, 2015), and constrained with ammonoid data from the overlying Flatsalen Formation (Korčinskaya, 1980; Smith, 1982).

3.c.4. Protodiploxypinus spp. Zone

Definition: The *Protodiploxypinus* spp. Zone was originally defined from the upper De Geerdalen Formation (Hopen Member) as the '*Protodiploxypinus* spp. Assemblage' by Paterson & Mangerud (2015). It is elevated to full zonal status here. The base of the zone is marked by an increased relative abundance of *Protodiploxypinus* spp., together with the first occurrence of several distinctive spore taxa including *Cingulizonates rhaeticus*, *Kyrtomisporis gracilis*, *K. laevigatus*, *K. speciosus*, *Limbosporites lundbladiae*, *Retitriletes austroclavatidites* and *Velosporites cavatus* (Fig. 4a). On Hopen, the *Protodiploxypinus* spp. Zone is also rich in fresh- to brackish-water algae, particularly *Plaesiodictyon mosellanum*. The top of the zone is defined by the decreased abundance of *Protodiploxypinus* spp., and the first common occurrence of *Classopollis torosus*, which delineates the base of the overlying *Classopollis torosus* Zone.

The assemblage is distinguished from the *Classopollis torosus* Zone by the high abundance of *Protodiploxypinus* spp. and *Plaesiodictyon mosellanum*, and the absence of *Classopollis* spp. The assemblage is distinguished from the underlying *Leschikisporis aduncus* Zone based on the relatively low abundance or absence of *Leschikisporis aduncus*.

Biozonal assemblages: *Araucariacites australis*, *Chasmatosporites apertus*, *C. hians*, *Cingulizonates rhaeticus*, *Concavisporites crassexinus*, *Cycadopites* spp., *Eucommiidites* spp., *Illinites chitonoides*, *Kyrtomisporis gracilis*, *K. laevigatus*, *K. speciosus*, *Limbosporites lundbladiae* (rare), *Ovalipollis ovalis*, *Plaesiodictyon mosellanum*, *Protodiploxypinus* spp., *Quadraeculina anellaeformis* (rare), *Retitriletes austroclavatidites*, *Ricciisporites umbonatus*, *Triadispora verrucata*, *Velosporites cavatus*, *Vesicaspora fuscus*, *Zebrasporites interscriptus* and *Z. laevigatus*. A representative selection of taxa from the zone is illustrated in Fig. 8.

Occurrence: The *Protodiploxypinus* spp. Zone has been recorded in preparations from the uppermost De Geerdalen Formation (Hopen Member) on Hopen (Paterson & Mangerud, 2015), Spitsbergen (Rismyhr *et al.* 2018) and in cores from the Sentralbanken High (Paterson *et al.* 2018). The zone has also been observed in Nordkapp Basin wells 7228/2-1s and 7228/9-1s (Paterson & Mangerud 2017).

Biostratigraphic correlation: The *Protodiploxypinus* spp. Zone is equivalent to the late Carnian 'Assemblage C' (Hochuli *et al.* 1989), 'Floral Phase 15' (Hochuli & Vigran, 2010, Fig. 2), the *Rhaetogonyaulax* spp. Zone (Vigran *et al.* 2014) and the *Protodiploxypinus ornatus* Composite Assemblage Zone (Rismyhr *et al.* 2018), all of which are characterized by the increased relative abundance of *Protodiploxypinus* spp. The *Protodiploxypinus* spp. Zone probably correlates with the upper part of the undifferentiated Carnian 'T_2k palynocomplex' of the Russian Barents Sea (Fig. 3). However, to the best of our knowledge, an increased abundance of *Protodiploxypinus* in the upper Carnian Russian deposits has not been recognized.

Age: The zone is dated as late Carnian (Tuvalian 3) based on magnetostratigraphic data from the De Geerdalen Formation on Hopen (Lord *et al.* 2014; Paterson & Mangerud, 2015), which is further constrained by an early Norian ammonoid fauna from the overlying Flatsalen Formation (Korčinskaya, 1980; Smith, 1982).

3.d. Norian

3.d.1. Classopollis torosus Zone

Definition: The *Classopollis torosus* Zone was first described as the '*Classopollis torosus* Assemblage' by Paterson & Mangerud (2015) based on assemblages from the lowermost Flatsalen Formation on Hopen. It is elevated to full zonal status here. The zone is defined by the first common occurrence of the pollen taxa *Classopollis torosus* (Fig. 4a, b). On Hopen, the zone is also characterized by the presence of microforaminiferal test-linings and the fresh- to brackish-water alga *Plaesiodictyon mosellanum*. Paterson & Mangerud (2015, fig. 13) suggested that the first occurrences of *Cavatoretisporites obvius* and *Retitriletes austroclavatidites* occurred within the zone; however, these taxa have been subsequently documented within the preceding

https://doi.org/10.1017/S0016756819000906 Published online by Cambridge University Press

Protodiploxypinus spp. Zone in the Sentralbanken area (e.g. Paterson *et al.* 2019*a*). Based on a compilation of available published data, the zone also contains the last occurrences of several long-ranging taxa including *Cordaitina minor*, *Illinites chitonoides*, *Kraeuselisporites cooksonae*, *Patinasporites densus*, *Staurosaccites quadrifidus*, *Triadispora verrucata*, *Voltziaceaesporites heteromorpha* and *Vallasporites ignacii*.

Biozonal assemblages: *Annulispora folliculosa*, *Cavatoretisporites obvius*, *Chasmatosporites apertus*, *C. hians*, *Cingulizonates rhaeticus*, *Classopollis torosus*, *Clathroidites papulosus*, *Deltoidospora* spp., *Kyrtomisporis gracilis*, *K. laevigatus*, *K. speciosus*, *Limbosporites lundbladiae* (rare/sporadic), *Polycingulatisporites bicollateralis*, *Protodiploxypinus* spp., *Quadraeculina anellaeformis* (rare/sporadic), *Retitriletes austroclavatidites*, *Rogalskaisporites cicatricosus*, *Zebrasporites interscriptus* and *Z. laevigatus*. A representative selection of taxa from the *Classopollis torosus* zone is illustrated in Figure 9.

Occurrence: Assemblages corresponding to the *Classopollis torosus* Zone have been recovered from outcrops of the Flatsalen Formation on Hopen (Paterson & Mangerud, 2015), Kong Karls Land (Smelror *et al.* 2019) and cores from the Sentralbanken High (Paterson *et al.* 2019*a*). The zone has also been described from the lower Fruholmen Formation in the Hammerfest and Nordkapp basins (in the latter, undifferentiated from the overlying *Rhaetogonyaulax rhaetica* Zone) (Paterson & Mangerud, 2017).

Biostratigraphic correlation: The *Classopollis torosus* Zone is tentatively correlated with 'Assemblage B-2' of Hochuli *et al.* (1989) and the lowermost part of the *Limbosporites lundbladii* Zone (Vigran *et al.* 2014) (Fig. 3). Comparable assemblages rich in *Classopollis torosus* have been recorded in areas of the Russian Barents Shelf within Norian 'T_3k-n palynocomplex' (Pavlov *et al.* 1985; Fefilova, 1988; Mørk *et al.* 1993).

Age: The *Classopollis torosus* Zone is dated as early Norian (Lacian) based on an ammonoid fauna from the Flatsalen Formation on Hopen, which includes *Argosirenites nelgechensis*, a form typical of the *Mojsisovicsites kerri* Zone of British Columbia (Korčinskaya, 1980; Smith, 1982).

3.d.2. Rhaetogonyaulax arctica Dinoflagellate Cyst Zone

Definition: The *Rhaetogonyaulax arctica* Dinoflagellate Cyst Zone is defined by the first common occurrence of the dinoflagellate cyst *Rhaetogonyaulax arctica*, which occurs in association with the common occurrence of microforaminiferal test linings. This event was originally applied by Paterson & Mangerud (2015) as a defining feature of their '*Classopollis torosus* Assemblage'. However, since the occurrence of dinoflagellate cysts is facies dependent and varies considerably across the region, separate spore-pollen and dinoflagellate cyst zones are now defined (Figs 3, 4a, b).

Biozonal assemblages: *Rhaetogonyaulax arctica* (common) and *R. rhaetica* (Fig. 9).

Occurrence: Assemblages belonging to this zone have been recorded from the transition between the De Geerdalen and lowermost Flatsalen formations on Spitsbergen, Hopen and in core material from the Sentralbanken High (Vigran *et al.* 2014; Paterson & Mangerud 2015; Paterson *et al.* 2019*a*; Rismyhr *et al.* 2018). Comparable assemblages have also been recovered from the lower Fruholmen Formation in the Hammerfest and Nordkapp basins (in the latter, undifferentiated from the overlying *Rhaetogonyaulax rhaetica* Dinoflagellate Cyst Zone) (Paterson & Mangerud 2017).

Biostratigraphic correlation: The zone essentially correlates with the *Rhaetogonyaulax arctica* Zone defined by Rismyhr *et al.* (2018) on Spitsbergen, which in turn was based on the marine component present in *Classopollis torosus* Assemblage of Paterson & Mangerud (2015).

Age: On Hopen, the zone is dated by an early Norian ammonoid fauna from the Flatsalen Formation, which includes *Argosirenites nelgechensis*, a taxon typical of the *Mojsisovicsites kerri* Zone of British Columbia (Korčinskaya, 1980; Smith, 1982). At the Festningen section on Spitsbergen, Vigran *et al.* (2014) proposed a tentative late Carnian – early Norian age for comparable assemblages. Since the occurrence of dinoflagellate cysts is facies dependent, it is probable that the base of the zone is diachronous, younging in a southeasterly direction towards the palaeoshoreline.

3.d.3. Rhaetogonyaulax rhaetica Dinoflagellate Cyst Zone

Definition: The *Rhaetogonyaulax rhaetica* Dinoflagellate Cyst Zone was first described as the '*Rhaetogonyaulax rhaetica* Assemblage' by Paterson & Mangerud (2015). It is elevated to full zonal status here and differentiated from the correlative spore-pollen zone (Fig. 3). The base of the zone is defined based on the first common to abundant occurrence of *R. rhaetica*, with occurrences of *Sverdrupiella* spp. (Fig. 4b). The top of the zone is defined by the last occurence of *R. rhaetica* and *Sverdrupiella* spp.

Biozonal assemblages: *Heibergella aculeata*, *H. asymmetrica*, *Noricysta fimbriata*, *N. varivallata*, *Rhaetogonyaulax arctica*, *R. rhaetica* (dominant) and *Sverdrupiella mutabilis*. A representative selection of taxa from the *Classopollis torosus*, *Rhaetogonyaulax arctica* and *R. rhaetica* zones are illustrated in Figure 9.

Occurrence: Assemblages assigned to the *Rhaetogonyaulax rhaetica* Dinoflagellate Cyst Zone are well represented in outcrop samples from the Flatsalen Formation on Hopen (Paterson & Mangerud, 2015) and Kong Karls Land (Smelror *et al.* 2019), and in core material from the Sentralbanken High (Paterson *et al.* 2018). However, in more proximal areas, such as in the Nordkapp Basin, it is more difficult to distinguish between the *Rhaetogonyaulax arctica* and *R. rhaetica* zones, due to the overall lower abundance of dinoflagellate cysts (Paterson & Mangerud 2017).

Biostratigraphic correlation: The *Rhaetogonyaulax rhaetica* Dinoflagellate Cyst Zone correlates with the marine components of 'Assemblage B-2' of Hochuli *et al.* (1989) and the lower part of the *Limbosporites lundbladii* Zone (Vigran *et al.* 2014). The *Rhaetogonyaulax rhaetica* Zone also likely correlates with the T_3n palynocomplex of the Russian Barents Shelf (Fig. 3). The *Rhaetogonyaulax rhaetica* Zone is equivalent to the *Heibergella* spp. Composite Assemblage Zone defined by Rismyhr *et al.* (2018) on Spitsbergen. However, the latter seems to be more taxonomically diverse due to its occurrence in a more distal depositional setting.

Comments: The *Rhaetogonyaulax rhaetica* Dinoflagellate Cyst Zone is distinguished from the *Rhaetogonyaulax* spp. Zone of Vigran *et al.* (2014), which was described from the uppermost De Geerdalen Formation (Isforden Member) at Festningen on Spitsbergen. The latter zone is likely an equivalent of our *Rhaetogonyaulax arctica* Zone described here, and is assigned a latest Carnian – early Norian age. Contrary to observations reported in Vigran *et al.* (2014, p. 74), common to abundant specimens of *R. rhaetica* were not recorded in assemblages from the uppermost De Geerdalen Formation in our subsequent analysis elsewhere on Svalbard or the Barents Shelf. However, since Festningen occupied a more distal position in the basin, it is possible that *R. rhaetica* has a longer range at that locality, with a first occurrence during the late Carnian Age.

Age: The *Rhaetogonyaulax rhaetica* Dinoflagellate Cyst Zone is dated as early Norian (Lacian) by an ammonoid fauna from the Flatsalen Formation on Hopen, which includes *Argosirenites*

https://doi.org/10.1017/S0016756819000906 Published online by Cambridge University Press

nelgechensis, a form typical of the *Mojsisovicsites kerri* Zone of British Columbia (Korčinskaya, 1980; Smith, 1982).

3.d.3. *Quadraeculina anellaeformis* Zone

Definition: The *Quadraeculina anellaeformis* Zone was originally defined as the informal '*Limbosporites lundbladii* – *Quadraeculina anellaeformis* Assemblage' by (Paterson & Mangerud, 2015). It is elevated to full zonal status here. The base of the zone is defined by the first consistent occurrence of *L. lundbladiae* and *Q. anellaeformis* (Fig. 4b) and the absence of dinoflagellate cysts and acritarchs, which characterize the preceding *Rhaetogonyaulax rhaetica* Dinoflagellate Cyst Zone. The latter feature is clearly facies controlled but seems to be related to a regionally significant regression, corresponding with the change from the marine shales of the Flatsalen Formation to the deltaic sandstones of the Svenskøya Formation (Paterson *et al.* 2016, 2019*a*). The top of the zone is defined by the base of the overlying *Ricciisporites* spp. Zone.

Biozonal assemblages: *Araucariacites australis*, *Chasmatosporites apertus*, *C. hians*, *Cycadopites* spp., *Deltoidospora* spp., *Kyrtomisporis gracilis*, *K. laevigatus*, *K. speciosus*, *Limbosporites lundbladiae* and *Quadraeculina anellaeformis*. A representative selection of taxa from the *Limbosporites lundbladii* and *Ricciisporites* spp. zones are illustrated in Figure 10.

Occurrence: The *Quadraeculina anellaeformis* Zone has been recorded in preparations from the lower part of the Svenskøya Formation on Hopen (Paterson & Mangerud, 2015) and Kong Karls Land (Smelror *et al.* 2019), and in stratigraphical cores from the Sentralbanken High (Paterson *et al.* 2019*a*). Assemblages corresponding to the zone have also been recorded in the middle part of the Fruholmen Formation in exploration wells in the Nordkapp Basin (Paterson & Mangerud 2017) (Fig. 3).

Biostratigraphic correlation: The *Quadraeculina anellaeformis* Zone correlates with the '*Limbosporites lundbladii* – *Quadraeculina anellaeformis* Assemblage' of Paterson & Mangerud (2015), which was described from the lower part of the Svenskøya Formation on Hopen. Equivalent assemblages have been documented in the Fruholmen Formation in exploration wells from the southern Barents Sea as 'assemblage SBS-II' (Paterson & Mangerud 2017), and from the Svenskøya Formation in stratigraphical cores from the Sentralbanken High (Paterson *et al.* 2018). The zone correlates with 'Assemblage B1' of Hochuli *et al.* (1989) and the upper part of the *Limbosporites lundbladii* Zone of Vigran *et al.* (2014). On Hopen, the *Quadraeculina anellaeformis* Zone corresponds to an interval rich in lycopsid megaspores, recently defined as the *Dijkstraisporites beutleri* – *Verrutriletes preutilis* Zone (Paterson *et al.* 2019*b*).

Age: Regionally, outcrops of the Svenskøya Formation (and correlative interval of the Fruholmen Formation) are devoid of age-diagnostic macrofossil remains. The presence of an early Norian ammonoid fauna in the underlying Flatsalen Formation (Korčinskaya, 1980; Smith, 1982) constrains the age of the Svenskøya Formation as Norian or younger; however, since the two formations are separated by an erosional unconformity, it is uncertain how much of the Norian is missing. In the absence of direct independent faunal control, a Norian–(?) Rhaetian age has been proposed (Paterson & Mangerud, 2015; Paterson *et al.* 2019*a*).

3.e. Rhaetian

3.e.1. *Ricciisporites* spp. Zone

Definition: The *Ricciisporites* spp. Zone is defined based on the first common occurrence of *Ricciisporites annulatus* and *R. tuberculatus*, with consistent occurrences of *Cerebropollenites* spp., *Rogalskaisporites ambientis*, *Polycingulatisporites crenulatus* and *P. mooniensis*. The top of the zone is marked by the last occurrences of several taxa including *Aratrisporites laevigatus*, *A. macrocavatus*, *Kyrtomisporis gracilis*, *K. laevigatus*, *K. speciosus*, *Limbosporites lundbladiae*, *Ovalipollis* spp., *Ricciisporites annulatus*, *R. tuberculatus* and taeniate bisaccate pollen.

Biozonal assemblages: *Aratrisporites* spp., *Baculatisporites* spp., *Cerebropollenites macroverrucosus*, *Chasmatosporites apertus*, *C. hians*, *Cingulizonates rhaeticus*, *Concavisporites crassexinus*, *Deltoidospora* spp., *Ischyosporites* sp., *Kyrtomisporis gracilis*, *K. laevigatus*, *K. speciosus*, *Limbosporites lundbladiae*, *Lunatisporites rhaeticus*, *Ovalipollis ovalis*, *Polycingulatisporites crenulatus*, *P. mooniensis*, *Quadraeculina anellaeformis*, *Ricciisporites annulatus*, *R. tuberculatus*, *Striatella parva*, *S. seebergensis*, *Trachysporites* spp., *Zebrasporites interscriptus* and *Z. laevigatus*.

Occurrence: Assemblages corresponding to the *Ricciisporites* spp. Zone have been recorded from the uppermost Svenskøya Formation on Hopen and in preparations from the Fruholmen Formation in exploration wells from the Nordkapp Basin (Paterson & Mangerud, 2015, 2017).

Comments: The *Ricciisporites* spp. Zone was previously described as the '*Rogalskaisporites ambientis* Assemblage' by Paterson & Mangerud (2015). Despite the probable correlation with the *Ricciisporites tuberculatus* Zone of Vigran *et al.* (2014), Paterson & Mangerud (2015) proposed *R. ambientis* as an alternative to the nominate taxon, due to the absence of *R. tuberculatus* on Hopen. Instead, assemblages on Hopen contained laevigate specimens more consistent with the taxonomic circumscription of *Ricciisporites annulatus*. Subsequent investigation of the correlative Fruholmen Formation in the Nordkapp Basin has shown both *R. annulatus* and *R. tuberculatus* to be present in the same assemblages, while *Rogalskaisporites ambientis* is absent. It is therefore possible that the distribution of each of these taxa is facies dependent.

The first consistent occurrence of *Cerebropollenites macroverrucosus* is also characteristic of this zone. The taxon has previously been considered diagnostic of the Jurassic (e.g. Vigran *et al.* 2014). However, co-occurrence of the taxon with *Aratrisporites* spp. and striate bisaccate pollen (e.g. Paterson & Mangerud, 2015) is suggestive of a Rhaetian age.

Biostratigraphic correlation: The *Ricciisporites* spp. Zone correlates with 'Assemblage A' of Hochuli *et al.* (1989) and the Rhaetian-aged *Ricciisporites tuberculatus* Zone of Vigran *et al.* (2014). The zone likely corresponds to the 'T_3r palynocomplex' of the Russian Barents Shelf (Fig. 3).

Age: Regionally, the Svenskøya Formation, and correlative interval of the Fruholmen Formation, lack age-diagnostic macrofossil remains. However, ammonoid data from the underlying Flatsalen Formation (Korčinskaya, 1980; Smith, 1982) constrains the age of the Svenskøya Formation as Norian or younger. Paterson & Mangerud (2015) proposed a tentative Rhaetian age for the zone, in agreement with previous interpretations by Hochuli *et al.* (1989) and Vigran *et al.* (2014).

4. Discussion

The palynozonation presented here provides an enhanced stratigraphical resolution for the Middle–Upper Triassic stratigraphy of the Norwegian Barents Sea, which builds upon the regional stratigraphic framework established by previous workers (e.g. Hochuli

https://doi.org/10.1017/S0016756819000906 Published online by Cambridge University Press

et al. 1989; Vigran *et al.* 2014). The primary contribution of this present work is in the refinement of the Late Triassic zonal scheme, which in the previous scheme was divided into four zones (Fig. 3) corresponding to a timespan of 35.6 Ma (e.g. Ogg *et al.* 2016). The recognition of seven spore-pollen zones thus improves the biozonal resolution for a key stratigraphic interval, which includes economically significant hydrocarbon source and reservoir units (Henricksen *et al.* 2011; Lundschien *et al.* 2014; Ryseth 2014). The results of this study therefore make an important contribution to ongoing exploration in the region. This is particularly true for Barents Sea North, an area not yet opened for exploration. In a recent evaluation of the region (NPD 2017) the Norwegian Petroleum Directorate estimates that Triassic reservoirs make the largest contribution to resource potential with no less than 56% of the area's recoverable resources. However, geological uncertainty is still high; the palynozonation presented here therefore provides much-needed age control in this relatively unexplored area.

The present work also contributes to a greater understanding of Triassic palynofloras on the northern Pangaean margin, which have been convincingly demonstrated to be taxonomically and quantitatively distinct from those of other areas such as the Germanic or Alpine regions. Several palynofloral trends have been noted, which likely reflect palaeoenvironment and, perhaps, palaeoclimatic control. These are briefly commented upon here; however, a more complete interpretation of their significance awaits further study, particularly in the Russian sector of the Barents Sea.

Firstly, the high abundance of *Aratrisporites* spp. in Anisian deposits of the Greater Barents Sea area is a feature which is recognized in coeval deposits of both the western (Hochuli & Vigran 2010; Vigran *et al.* 2014; Paterson & Mangerud 2017) and eastern regions (Pavlov *et al.* 1985; Mørk *et al.* 1993; Fefilova, 2013). This particular genus has been recovered *in situ* in sporangial remains of various heterosporous lycopsids of the families Isoetaceae and Pleuromeiaceae (Balme, 1995; Taylor *et al.* 2009), which likely grew in coastal lagoons or mangrove-type habitats (Retallack, 1975, 1997; Kürschner & Herngreen, 2010). As noted by Hochuli & Vigran (2010), in lower palaeolatitudes this taxon is particularly common in assemblages with other evidence for high humidity (c.f. Hochuli & Frank, 2000). The apparent uniformity in Anisian palynofloras across the Greater Barents Sea suggests that the area comprised a single flora province during that time. These Anisian assemblages contrast with those described from central and southern European localities, where assemblages are composed almost exclusively of xerophytic taxa such as *Triadispora*, considered indicative of arid palaeoclimatic conditions (e.g. Kürschner & Herngreen, 2010). Nonetheless, some differences are apparent between Anisian palynofloras from the western and eastern Barents Sea. For instance, there is a marked increase in bisaccate pollen and acritarchs in deposits of Svalbard and the Norwegian Barents Sea that is not recognized in the Russian sector (Mørk *et al.* 1993). This likely reflects the fact that much of western Barents Sea was situated in a more distal basinal setting during this time, while the eastern sector was dominated by an extensive coastal plain (Lundschien *et al.* 2014; Klausen *et al.* 2015). The influx in bisaccate pollen in the Norwegian Barents Sea during the Anisian may therefore be due to the 'Neves effect' of Chaloner & Muir (1968).

The almost total dominance of *Leschikisporis aduncus* is a common feature in upper Carnian De Geerdalen on Svalbard and in the correlative upper Snadd Formation in many areas of the Barents Sea (Hochuli & Vigran, 2010; Vigran *et al.* 2014; Paterson & Mangerud, 2015, 2017; Paterson *et al.* 2017, 2019*a*). This spore has been isolated from fertile fronds of the fern *Asterotheca merianii* (Bhardwaj & Singh, 1957; Vasilevskaya, 1972; Kustatscher & Van Konijnenburg-van Cittert, 2011), which is equally prevalent among late Carnian macrofloras from Svalbard (Pott, 2014). Based on the size of several *A. merianii* fossils, Pott (2014) argued that these plants may have been quite tall 'tree-like' ferns, similar to modern *Dicksonia* species. The plant is interpreted to have grown in humid swamp habitats (Roghi *et al.* 2010), which is consistent with the dominance of *L. aduncus* in coal layers on Svalbard (Bjærke & Manum, 1977; Vigran *et al.* 2014; Paterson & Mangerud, 2015). The wide distribution of assemblages belonging to the *L. aduncus* Zone in the western Barents Sea region suggests the establishment of a vast coastal plain swamp. Intriguingly, this coincides with the maximum regressive phase of the De Geerdalen deltaic system (Klausen *et al.* 2015). Paterson *et al.* (2015) interpreted the dominance of *L. aduncus* to reflect the basinwards expansion of humid coastal plain habitats accompanying this marine regression. The co-occurrence of certain pollen taxa typically considered indicative of drier conditions, such as *Ovalipollis*, in assemblages of the *Leschikisporis aduncus* Zone probably reflects an allochthonous palynoflora transported by wind and rivers from the hinterland.

The abrupt transition to the *Protodiploxypinus* Zone in uppermost Carnian strata marks the disappearance of *L. aduncus* in the western Barents Sea, and the replacement of fern-spore-dominated palynofloras by assemblages rich in *Protodiploxypinus* and the alga *Plaesiodictyon mosellanum*. *Protodiploxypinus* was produced by a xerophytic coastal pioneer plant (Brugman *et al.* 1994), while *P. mosellanum* is thought to reflect fresh- to brackish-water habits (Brenner, 1992; Brenner & Foster, 1994; Wood & Miller, 1998; Wood & Benson, 2000). On Hopen, the palynofloral turnover coincides with a marine transgression (Lord *et al.* 2014), leading Paterson *et al.* (2015) to propose that it was driven by an inundation of coastal plain habitats by brackish water, resulting in the destruction of the habitats in which *Asterotheca meriani* was growing. This interpretation is consistent with the continued presence of *L. aduncus* in the Rhaetian in the more proximal eastern region of the Barents Sea (e.g. Mørk *et al.* 1993; Fefilova, 2013); its disappearance in the Norwegian Barents is therefore apparently local, and driven by palaeoenvironmental rather than climatic change.

The uppermost Carnian *Protodiploxypinus* spp. Zone is also notable for the first occurrence of the fern spores *Kyrtomisporis gracilis*, *K. laevigatus* and *K. speciosus*, the lycopsid spore *Retitriletes austroclavatidites* and the pollen taxon *Quadraeculina anellaeformis*. In central and southern European localities, these taxa do not typically appear until the Rhaetian Age (e.g. Cirilli, 2010; Kürschner & Herngreen, 2010); their first occurrence in the Barents Sea therefore apparently occurs *c.* 20 Ma earlier than elsewhere. We postulate that these taxa first evolved on the northern coastline of Pangaea during the late Carnian Age, perhaps in response to the palaeoenvironmental and palaeoecological change triggered by rising sea levels. The taxa then spread to most of central and southern Europe by the Rhaetian Age during a humid phase.

The influx of *Classopollis* pollen during early Norian time in both the western (Vigran *et al.* 2014; Paterson & Mangerud 2015; Paterson *et al.* 2016) and eastern sectors of the Barents Sea (Pavlov *et al.* 1985; Fefilova, 1988; Mørk *et al.* 1993) corresponds to a regionally marine transgression (i.e. the S6/N1 sequence boundary of Klausen *et al.* 2015). The increase in *Classopollis* may therefore reflect the spread of halophytic conifers (see Alvin, 1982; Abbink *et al.* 2004), which colonized tidal flat

https://doi.org/10.1017/S0016756819000906 Published online by Cambridge University Press

environments created by rising relative sea levels. However, since an increase in Circumpolles including *Classopollis* is also a common feature of lower Norian assemblages from lower palaeolatitudes (Lund 1977; Schuurman 1977, 1979; Orłowska-Zwolińska 1985; Kürschner & Herngreen, 2010; Fijałkowska-Mader *et al.* 2015), their proliferation may be of wider palaeoclimatic significance.

5. Systematic palynology

Genus *Kyrtomisporis* (Mädler) Van der Eem, 1983

Type species *Kyrtomisporis laevigatus* Mädler, 1964

Kyrtomisporis moerki sp. nov. Figure 6b.

2017 *Kyrtomisporis* sp. A; Paterson, Mangerud & Mørk, pl. 2, 12–15.

2017 *Kyrtomisporis* sp. A; Paterson & Mangerud, fig. 3.

2019*a* *Kyrtomisporis* sp. A; Paterson, Mangerud, Holen, Landa, Lundschien & Eide, pl. 2, M.

Derivation of name. Named after the Norwegian geologist Dr Atle Mørk in recognition of his contribution to Triassic stratigraphy and sedimentology in the Norwegian Arctic.

Holotype. PMO 234.376 B, core 7830/5-U-1, 68.82 m depth (slide A), England Finder slide coordinates M44-1, Figure 6b.

Paratypes. Core 7830/5-U-1: PMO 234.385 A, 68.82 m depth (slide B), England Finder slide coordinates V53-1, Figure 11k; PMO 234.376 C, 68.82m depth (slide A), England Finder slide coordinates Q40-1, Figure 11l; PMO 234.376 A, 68.82m depth (slide A), England Finder slide coordinates K40-4, Figure 11m.

Diagnosis. Trilete spores, kyrtomate and cingulate. Amb roundly triangular with convex interradials. Laesurae simple, slightly sinuous and bordered by narrow labra extending to inner margins of cingulum. Proximal face with kyrtome, fusing with cingulum at apices; kyrtome 8–(13)–20 µm at the narrowest point and 12–(19)–25 µm wide at the widest point. Proximal and distal surface densely ornamented with an apiculate sculpture consisting of verrucae, pila and spinules. Sculptural elements 0.5–(1.2)–1.8 µm wide, 0.6–(1.4)–6 µm tall, projecting along the margins of the amb and kyrtome. Cingulum 3–(7)–12 µm wide, faint, often obscured by the dense ornament.

Description. A species of *Kyrtomisporis* that is characterized by a scabrate–apiculate ornament on both proximal and distal faces. Proximal surface with arcuate thickenings in the interradial areas, bordering the laesurae. In some specimens the thickenings form simple tori; however, in most specimens the thickenings comprise a true kyrtome which extends to the cingulum at the apices, where they occasional form circular, button-like protrusions, as present in other members of the genus. Spores also observed as rare tetrads.

Dimensions. 54–(64)–80 µm (based on 25 measured specimens).

Type locality. Stratigraphic core 7830/5-U-1, offshore Kong Karls Land, Barents Sea.

Type stratum. Snadd Formation (lower De Geerdalen Formation equivalent).

Age. Late Triassic (early Carnian).

Comparison. *Kyrtomisporis moerki* sp. nov. is distinguished from all other members of the genus by its scabrate to apiculate ornament on both proximal and distal surfaces. *Kyrtomisporis ervii* Van der Eem, 1983 and *K. pseudoreticulatus* Sivak & Shang, 1989 are characterized by a distal ornament of irregular rugulae, often perpendicular to the interradials. *Kyrtomisporis coronarius* (Chang) Li & Shang, 1980 and *K. gracilis* Bjærke and Manum, 1977, have a radially rugulate ornament, with large bulbous projections along the amb in equatorial view. *Kyrtomisporis corrugatus* Cameron, 1974 is distinguished by its strongly crenulated cingulum. *Kyrtomisporis laevigatus* Mädler, 1964 is distinguished by its sparse distal ornament of broad-based, low verrucae. *Kyrtomisporis speciosus* Mädler, 1964 has a dense verrucate, papillate to coalescent rugulate ornament. *Kyrtomisporis niger* Bjærke & Manum, 1977 is characterized by a chagrenate to laevigate surface, and a distal face with five to seven low, faint transverse ridges, 3–5 µm wide. *Concavisporites scabratus* Bjærke & Manum, 1977 is superficially similar to *Kyrtomisporis moerki* sp. nov. based on its tori and scabrate ornament, but is acingulate and has a smooth outer surface in optical section. *Habrozonosporites* Lu & Wang, 1980 possesses a kyrtome and has a similar ornament, but is camerate and acingulate.

Genus *Semiretisporis* Reinhardt, 1962

Type species: *Semiretisporis gothae* Reinhardt, 1962

Semiretisporis hochulii sp. nov. Figures 5d, 10a–f.

1985 '*Semiretisporis barentszi*' van Veen, p. 98–99, pl. 9, 7; pl. 10, 7, 8, 10, pl. 11, 1.

1989 *Semiretisporis* sp. 1 Hochuli, Colin & Vigran, pl. 4, 1,2, p. 142.

1998 *Semiretisporis* sp. A Vigran, Mangerud, Mørk, Bugge & Weitschat, pl. 9, 1.

2008 *Semiretisporis* sp. 1 '*barentzii*' Hounslow, Yu, Mørk, Weitschat, Vigran, Karloukovski & Orchard, fig. 7.

2014 '*Semiretisporis barentzii*' Vigran, Mangerud, Mørk, Worsley & Hochuli, p. 82, 150, 154, 155, 173, 175, 263.

2014 '*Semiretisporis* sp. A *(barentzii)*' Vigran, Mangerud, Mørk, Worsley & Hochuli, p. 90, 97, 98, 143, 149, 263; pl. 18, I.

Holotype. PMO 234.369 A, core 7534/4-U-1, 189.66 m depth, England Finder slide coordinates K54, Figure 5d.

Paratypes. Core 7534/4-U-1: PMO 234.367 A, 171.83 m depth, 5B, England Finder slide coordinates C45-4, Figure 11a; PMO 234.367 B, 171.83 m depth, 5B, England Finder slide coordinates K61, Figure 11b; PMO 234.372 E, 194.53 m depth, 7B, England Finder slide coordinates U41-4, Figure 11c; PMO 234.368 B, 175.10 m depth, 6B, England Finder slide coordinates G45, Figure 11d; PMO 234.368 A, 175.10 m depth, 6B, England Finder slide coordinates F46-4, Figure 11e; PMO 234.367 C, 171.83 m depth, 5B, England Finder slide coordinates O49, Figure 11f.

Derivation of name: The species is named in honour of the late Swiss palynologist Peter A. Hochuli in recognition of his contribution to Triassic palynology in the Barents Sea region.

Diagnosis: Trilete, cingulizonate, semireticulate spores. Amb triangular to subtriangular, with an irregular, often serrated outline. Trilete mark indistinct. Proximal surface essentially smooth. Distal surface sparsely ornamented with baculae, verrucae and echinae, which on some specimens coalesce into a loosely defined reticulum. Ornament more densely concentrated on the equator, fusing to form a cingulum (4–16 µm wide), bordered by a zona (7–18 µm wide). Narrow, digitate rugulae, 2–7 µm wide, radiate from the cingular thickening, and fuse with the outer margin of the zona, delineating lumina 3–8 µm wide.

Description: A species of *Semiretisporis* that is characterized by a combination of verrucate, echinate and baculate sculptural elements, which fuse to form a cingulum, from which narrow rugulae radiate, merging with the outer margins of a zona. The ornament defines a loose and inconsistently developed reticulate pattern. The density, size and distribution of the sculptural

https://doi.org/10.1017/S0016756819000906 Published online by Cambridge University Press

elements and degree of reticulum connectivity varies considerable between specimens, as does the overall equatorial spore diameter, and zona and cingulum width.

Dimensions. Total diameter 58–(69)–86 µm; inner body 26–(33)–45 µm (based on 22 measured specimens).

Type locality: Stratigraphical core 7534/4-U-1, Sentralbanken High, Barents Sea.

Type horizon: lower Snadd Formation.

Stratigraphic range: Ladinian – lower Carnian (*Echinitosporites iliacoides–Podosporites vigraniae* zones).

Comparison: *Semiretisporis hochulii* sp. nov. is distinguished from *S. gothae* Reinhardt 1962, and *S. maljavkinae* Schulz 1967, due to the more irregular nature of its reticulum and zona margin.

Comment: This species was informally described as *Semiretisporis 'barentszi'* by van Veen (1985). However, the name was not effectively published based on ICBN Article 30.9 and Note 3, Recommendation 30A.4 (Turland *et al.* 2018). Furthermore, no holotype was designated in van Veen's description.

Genus: *Podosporites*

Type species: *Podosporites tripakshi* Rao, 1943

Podosporites vigraniae sp. nov. Figures 5k, 6n, 11g–j.

Holotype. PMO 234.374 B, core 7534/4-U-1, 216.09 m depth, England Finder slide coordinates S42-2, Figure 5k.

Paratypes. PMO 234.379 A, core 7830/5-U-1, 91.57 m depth (slide B), England Finder slide coordinates G47-1, Figure 6n; PMO 234.394 C, core 7533/2-U-1, 164.75 m depth, England Finder slide coordinates D49-2, Figure 11g; PMO 234.383 E, core 7830/5-U-1, 126.94 m depth (slide A), England Finder slide coordinates F44-1, Figure 11h; PMO 234.372 B, core 7534/4-U-1, 194.53 m depth, 7B, England Finder slide coordinates E37-4, Figure 11i; PMO 234.392 E, core 7533/2-U-1, 157.98 m depth, England Finder slide coordinates L61-4, Figure 11j.

Derivation of name: The species is named after the Norwegian palynologist Jorunn Os Vigran, in recognition of her contributions to Triassic palynostratigraphy in the Barents Sea region.

Diagnosis: Bisaccate or trisaccate, monosulcate pollen. Central body circular or oval in shape. Sacci rudimentary, situated on distal surface, forming low, sinuous or vermiculate ridges bordering a broad sulcal opening. Sulcus circular to oval in shape. Exine thick (3–6 µm) with a granulate to verrucate texture.

Description: A large species of *Podosporites* characterized by a thick wall, and poorly developed sacci. The sacci are displaced to the distal surface, where they form sinuous to vermiculate (occasionally straight) ridges 3–(4)–8 µm in width and height, which border the sulcus. Sulcal opening commonly gaping, 7–(17)–26 µm in width at the widest point. The exine is coarsely ornamented by granulae or low verrucae. Specimens are rarely folded due to the robust wall.

Dimensions. 50–(57)–77 µm width; 42–(53)–74 µm height (based on 15 measured specimens).

Type locality: Stratigraphical core 7534/4-U-1, Sentralbanken High, Barents Sea.

Type horizon: Snadd Formation (lower De Geerdalen Formation equivalent).

Stratigraphic range: Upper Anisian – upper Carnian (*Protodiploxypinus decus – Leschikisporis aduncus* zones).

Comparison: *Podosporites vigraniae* sp. nov. is closely comparable to *P. amicus* Scheuring, 1970, which was described from the Carnian Gipskeuper of Switzerland. However, according to Scheuring (1970) *P. amicus* is smaller (38–43 µm width; 30–38 µm height) with a thinner wall (2–3 µm). *Podosporites vigraniae* sp. nov. is therefore distinguished by its consistently larger size, thicker wall and coarser ornamentation.

Acknowledgements. This research was funded by a Forum for Reservoir Characterization, Reservoir Engineering and Exploration Technology Cooperation (FORCE) industry consortium, consisting of AkerBP (formerly Det Norske), Centrica, Chevron, ConocoPhillips, Dong, Eni, Lundin, Shell and Statoil. Niall W. Paterson received additional funding from the Norwegian Research Council through the 'Internal and external forcing factors on the source-to-sink infill dynamics of the Lower Mesozoic Greater Barents Sea Basin' (ISBAR) project (grant no. 267689). Both authors thank Malcolm Jones (Palynological Laboratory Services Limited) for preparation of palynological slides. The Norwegian Petroleum Directorate (NPD) and Applied Petroleum Technology are thanked for providing access to palynological preparations, exploration well samples and stratigraphical cores used in this study.

Declaration of Interest. The authors report no potential conflicts of interest.

References

Abbink OA, Van Konijnenburg-Van Cittert JHA and Visscher H (2004) A sporomorph ecogroup model for the Northwest European Jurassic – Lower Cretaceousi [sic]: concepts and framework. *Netherlands Journal of Geosciences* **83** (1), 17–38.

Alvin KL (1982) Cheirolepidiaceae: biology, structure and paleoecology. *Review of Palaeobotany and Palynology* **37**, 71–98.

Balme B (1995) Fossil in-situ spores and pollen grains: an annotated catalogue. *Review of Palaeobotany and Palynology* **87**, 81–323.

Benton MJ, Bernardi M and Kinsella C (2018) The Carnian Pluvial Episode and the origin of dinosaurs. *Journal of the Geological Society* 175(6), 1019, https://doi.org/10.1144/jgs2018-049

Bernardi M, Gianolla P, Petti FM, Mietto P and Benton MJ (2018) Dinosaur diversification linked with the Carnian Pluvial Episode. *Nature Communications* **9**, 1499, doi: 10.1038/s41467-018-03996-1.

Bhardwaj DC and Singh HP (1957) *Asterotheca meriani* (Brongn.) Stur and its spores from the Upper Triassic of Lunz (Austria). *The Palaeobotanist* **5**, 51–5.

Bjærke T (1977) Mesozoic palynology of Svalbard – II. Palynomorphs from the Mesozoic sequence of Kong Karls Land. *Norsk Polarinstitutt Årbok* **1976**, 83–120.

Bjærke T and Dypvik H (1977) Sedimentological and palynological studies of Upper Triassic – Lower Jurassic sediments in Sassenfjorden, Spitsbergen. *Norsk Polarinstitutt Skrifter* **165**, 1–48.

Bjærke T and Manum SB (1977) Mesozoic palynology of Svalbard – I. The Rhaetian of Hopen, with a preliminary report on the Rhaetian and Jurassic of Kong Karls Land. *Norsk Polarinstitutt Skrifter* **165**, 1–48.

Boucot AJ, Xu C, Scotese CR and Morley RJ (2013) *Phanerozoic Paleoclimate: An Atlas of Lithologic Indicators of Climate.* Society for Sedimentary Geology, Tulsa, OK, SEPM Concepts in Sedimentology and Paleontology, No. **11**, 478 pp.

Brenner W (1992) First results of Late Triassic palynology of the Wombat Plateau, Northwestern Australia. *Proceedings of the ODP, Scientific Results* **122**, 413–26.

Brenner W and Foster CB (1994) Chlorophycean algae from the Triassic of Australia. *Review of Palaeobotany and Palynology* **80** (3–4), 209–34.

Brugman WA, Van Bergen PR and Kerp JHF (1994) A quantitative approach to Triassic palynology: the Lettenkeuper of the Germanic Basin as an example. In *Sedimentation of Organic Particles* (ed A. Traverse), pp. 409–29. Cambridge University Press, Cambridge.

Cameron DK (1974) New Triassic palynomorphs from the Arabian Peninsula. *Grana* **14**, 4–10.

Chaloner WG and Muir M (1968) Spores and floras. In *Coal and Coal-Bearing Strata* (eds DS Murchison and TS Westoll), pp. 127–46. Oliver and Boyd, Edinburgh.

Cirilli S (2010) Upper Triassic–lowermost Jurassic palynology and palynostratigraphy: a review. In *The Triassic Timescale* (ed. SG Lucas), pp. 285–314. Geological Society of London, Special Publication no. **334**.

https://doi.org/10.1017/S0016756819000906 Published online by Cambridge University Press

Dallmann WK (1999) *Lithostratigraphic lexicon of Svalbard: review and recommendations for nomenclature use*. Committee on the Stratigraphy of Svalbard, Norwegian Polar Institute, Tromsø, 318 pp.

Eide CH, Klausen TG, Katkov D, Suslova AA and Helland-Hansen W (2018) Linking an Early Triassic delta to antecedent topography: Source-to-sink study of the southwestern Barents Sea margin. *GSA Bulletin* **130** (1/2), 263–83.

Fefilova LA (1988) Palinologicheskiye kompleksy triasovikh otlozheniy Barentseva shelfa (The palynological complexes of Triassic rocks of the Barents Shelf Plate). In *Barentsevomorskaja shelfovaya plita (Barents Shelf Plate)* (ed. IS Gramberg), pp. 149–51. Sb. Nauchn. Tr., PGO Sevmorgeologiya Vserossijskij Naučno-Issledovatel'skij Institut Geologii I Mineral'nyh Resursov Mirovogo Okeana (VNIIOkeanologiya), Leningrad [in Russian].

Fefilova LA (2001) Miospory iz triasovykh otlozheniy tsentral'noy chasti o. Zapadnyy Shpitsbergen (Sassen-f'ord, yuzhnoye poberezh'ye) (Triassic miospores from the central part of West Svalbard (Sassenfjord, south coast)). In *Biostratigrafiya mezozoya i kaynozoya nekotorykh regionov Arktiki i Mirovogo okeana (Biostratigraphy of the Mesozoic and Cenozoic of some regions of the Arctic and the World Ocean)* (ed. VA Basov), pp. 5–19. Vserossijskij Naučno-Issledovatel'skij Institut Geologii I Mineral'nyh Resursov Mirovogo Okeana (VNIIOkeanologiya), St Petersburg [in Russian].

Fefilova LA (2013) Biostratigrafiya, miospory i makroflora triasovykh otlozheniy yugo-vostochnoy chasti shel'fa Barentseva morya na primere Krestovoy ploshchadi i sopredel'nykh rayonov (Biostratigraphy, miospores and macroflora of Triassic sediments of the southeastern part of the Barents Sea shelf with the example of Krestovaya Field and adjacent areas). In *Materialy po biostratigrafii, faune i flore fanerozoya Rossii, Atlantiki i Antraktidy* (Materials on the biotostratigraphy, fauna and flora of the Phanerozoic of Russia, the Atlantic and the Antractic) (ed. LV Nekhorosheva), pp. 42–83. Naučno-Issledovatel'skij Institut Geologii Arktiki-Vserossijskij Naučno-Issledovatel'skij Institut Geologii I Mineral'nyh Resursov Mirovogo Okeana (NIIGA-VNIIOkeangeologiya), St Petersburg [in Russian].

Fijałkowska-Mader A, Heunisch C and Szulc J (2015) Palynostratigraphy and palynofacies of the Upper Silesian Keuper (Southern Poland). *Annales Societatis Geologorum Poloniae* **85**, 637–661.

Furin S, Preto N, Rigo M, Roghi G, Gianolla P, Crowley JL and Bowring SA (2006) High-precision U-Pb zircon age from the Triassic of Italy: implications for the Triassic time scale and the Carnian origin of calcareous nannoplankton and dinosaurs. *Geology* **34** (12), 1009–12.

Glørstad-Clark E, Birkeland EP, Nystuen JP, Faleide JI and Midtkandal I (2011) Triassic platform-margin deltas in the western Barents Sea area. *Marine and Petroleum Geology* **28**, 1294–314.

Glørstad-Clark E, Faleide JI, Lundschien BA and Nystuen JP (2010) Triassic sequence stratigraphy and paleogeography of the western Barents Sea area. *Marine and Petroleum Geology* **27**, 1448–75.

Henricksen E, Ryseth AE, Larssen GB, Heide T, Rønning K and Stoupakova AV (2011) Tectonostratigraphy of the greater Barents Sea: implications for petroleum systems. In *Arctic Petroleum Geology* (eds AM Spencer, AF Embry, DL Gautier, AV Stoupakova and K Sørensen), pp. 163–95. Geological Society of London, Memoir no. **35**,

Hochuli PA, Colin PA and Vigran JO (1989) Triassic biostratigraphy of the Barents Sea area. In *Correlation in Hydrocarbon Exploration* (ed. J Collinson), pp. 131–53. Graham and Trotman, London.

Hochuli PA and Frank SM (2000) Palynology (dinoflagellate cysts, sporepollen) and stratigraphy of the Lower Carnian Raibl Group in the Eastern Swiss Alps. *Eclogae Geologicae Helvetiae* **93**, 429–43.

Hochuli PA and Vigran JO (2010) Climate variations in the Boreal Triassic – Inferred from palynological records from the Barents Sea. *Palaeogeography, Palaeoclimatology, Palaeoecology* **290**, 20–42.

Hounslow MW, Yu M, Mørk A, Weitschat W, Vigran JO, Karloukovski V and Orchard MJ (2008) Intercalibration of Boreal and Tethyan time scales: the magnetobiostratigraphy of the Middle Triassic and the latest Early Triassic from Spitsbergen, Arctic Norway. *Polar Research* **27** (3), 469–90.

Høy T and Lundschien BA (2011) Triassic deltaic sequences in the northern Barents Sea. In *Arctic Petroleum Geology* (eds AM Spencer, AF Embry, DL Gautier, AV Stoupakova and K Sørensen), pp. 249–60. Geological Society of London, Memoir no. **35**.

Klaus W (1960) Sporen der karnischen Stufe der ostalpinen Trias. *Jahrbuch der Geologischen Bundesanstalt* **5**, 107–182, plates 28–38.

Klausen TG, Nyberg B and Helland-Hansen W (2019) The largest delta plain in Earth's history. *Geology* **47** (5), 470–74.

Klausen TG, Ryseth AE, Helland-Hansen W, Gawthorpe R and Laursen I (2015) Regional development and sequence stratigraphy of the Middle to Late Triassic Snadd Formation, Norwegian Barents Sea. *Marine and Petroleum Geology* **62**, 102–22.

Korčinskaya MV (1980) Rannenorijskaja fauna arhipelaga Sval'bard [Early Norian fauna of the archipelago of Svalbard]. In *Geologija osadočnogo čëhla arhipelaga Sval'bard [Geology of the Sedimentary Platform Cover of the Archipelago of Svalbard]* (ed. DV Semevskij), pp. 30–43. Naučno-Issledovatel'skij Institut Geologii Arktiki (NIIGA), Leningrad [in Russian].

Kürschner WM and Herngreen GFW (2010) Triassic palynology of central and northwestern Europe: a review of palynofloral diversity patterns and biostratigraphic subdivisions. In *The Triassic Timescale* (ed. SG Lucas), pp. 263–83. Geological Society of London, Special Publication no. **334**.

Kustatscher E and Van Konijnenburg-Van Cittert JHA (2011) The ferns of the Middle Triassic flora from Thale (Germany). *Neues Jahrbuch für Geologie and Paläontologie, Abhandlungen* **261**, 209–48.

Li W-B and Shang Y-K (1980) Sporo-pollen assemblages from the Mesozoic Coal Series of western Hubei Province, China. *Acta Palaeontologica Sinica* **19** (3), 201–19, 4 plates [in Chinese with English summary].

Lord GS, Solvi KH, Ask M, Mørk A, Hounslow MW and Paterson NW (2014) The Hopen Member: A new lithostratigraphic unit on Hopen and equivalent to the Isfjorden Member of Spitsbergen. *Norwegian Petroleum Directorate Bulletin* **11**, 81–96.

Lu M-N and Wang R-S (1980) The discovery of microflora from the Maantang Formation in the North-West Sichuan Basin and its significance. *Journal of Integrative Plant Biology* **22** (4), 370–78, 3 plates.

Lund JJ (1977) Rhaetic to Lower Liassic palynology of the onshore southeastern North Sea Basin. *Danmarks Geologiske Undersøgelse* **109**, 1–129.

Lundschien BA, Høy T and Mørk A (2014) Triassic hydrocarbon potential in the Northern Barents Sea; integrating Svalbard and stratigraphic core data. *Norwegian Petroleum Directorate Bulletin* **11**, 3–20.

Mädler K (1964) Bemerkenswerte Sporenformen aus dem Keuper und unteren Lias. *Fortschritte in der Geologie von Rheinland und Westfalen*, **12**, 169–200.

Mangerud G, Paterson NW and Riding JB (2018) The temporal and spatial distribution of Triassic dinoflagellate cysts. *Review of Palaeobotany and Palynology* 261, 53–66, doi: 10.1016/j.revpalbo.2018.11.010

Morbey SJ (1975) The palynostratigraphy of the Rhaetian stage, Upper Triassic in the Kendelbachgraben, Austria. *Palaeontographica B* **152**, 1–75.

Mørk A, Dallman WK, Dypvik H, Johannessen EP, Larssen GB, Nagy J, Nøttvedt A, Olaussen S, Pčhelina TM and Worsley D (1999) Mesozoic lithostratigraphy. In *Lithostratigraphic Lexicon of Svalbard, Upper Palaeozoic to Quaternary Bedrock: Review and Recommendations for Nomenclature Use* (ed. WK Dallman), pp. 127–241. Committee on the Stratigraphy of Svalbard, Norwegian Polar Institute, Tromsø.

Mørk A, Vigran JO and Hochuli PA (1990) Geology and palynology of the Triassic succession of Bjørnøya. *Polar Research* **8**, 141–63.

Mørk A, Vigran JO, Korchinskaya MV, Pchelina TM, Fefilova LA, Vavilov MN and Weitschat W (1993) Triassic rocks in Svalbard, the Arctic Soviet islands and the Barents Shelf: bearing on their correlations. In: *Arctic Geology and Petroleum Potential* (eds TO Vorren, E Bergsager, ØA Dahl-Stamnes, E Holter, B Johansen, E Lie and TB Lund), pp. 457–79. Norwegian Petroleum Society, Special Publication no. 2.

Mueller S, Hounslow MW and Kürschner WM (2016) Integrated stratigraphy and palaeoclimate history of the Carnian Pluvial Event in the Boreal realm; new data from the Upper Triassic Kapp Toscana Group in central Spitsbergen (Norway). *Journal of the Geological Society* **173** (1), 186–202.

NPD (2017) Geological assessment of petroleum resources in eastern parts of Barents Sea North 2017. Norwegian Petroleum Directorate, 1–39, https://www.npd.no/globalassets/1-npd/publikasjoner/rapporter-en/geologivurderingbhn-engelsk-lavoppl.pdf.

Ogg JG, Ogg GM and Gradstein FM (2016) *A Concise Geologic Time Scale*. Elsevier, Amsterdam, 234 pp.

https://doi.org/10.1017/S0016756819000906 Published online by Cambridge University Press

Orłowska-Zwolińska T (1985) Palynological zones of the Polish epicontinental Triassic. *Bulletin of the Academy of Sciences, Earth Sciences* **33**, 107–19.

Paterson NW and Mangerud G (2015) Late Triassic (Carnian – Rhaetian) palynology of Hopen, Svalbard. *Review of Palaeobotany and Palynology* **220**, 98–119.

Paterson NW and Mangerud G (2017) Palynology and depositional environments of the Middle – Late Triassic (Anisian – Rhaetian) Kobbe, Snadd and Fruholmen formations, southern Barents Sea, Arctic Norway. *Marine and Petroleum Geology* **86**, 304–24.

Paterson NW, Mangerud G, Cetean CG, Mørk A, Lord GS, Klausen TG and Mørkved PT (2016) A multidisciplinary biofacies characterisation of the Late Triassic (late Carnian–Rhaetian) Kapp Toscana Group on Hopen, Arctic Norway. *Palaeogeography, Palaeoclimatology, Palaeoecology* **464**, 16–42 (special issue: Mesozoic Ecosystems – Climate and Biota).

Paterson NW, Mangerud G, Holen LH, Landa J, Lundschien BA and Eide F (2019a) Late Triassic (early Carnian–Norian) palynology of the Sentralbanken High, Norwegian Barents Sea. *Palynology* 43 (1), 53–75, https://doi.org/10.1080/01916122.2017.1413018

Paterson NW, Mangerud G and Mørk A (2017) Late Triassic (early Carnian) palynology of shallow stratigraphical core 7830/5-U-1, offshore Kong Karls Land, Norwegian Arctic. *Palynology* **41** (2), 230–54.

Paterson NW, Morris PH and Mangerud G (2019b) Lycopsid megaspores from the Upper Triassic of Svalbard and their relationship to the floras and palaeoenvironments of Northern Pangaea. *Papers in Palaeontology*, published online 14 February 2019, https://doi.org/10.1002/spp2.1251

Pavlov VV, Fefilova LA and Lodkina LB (1985) Palinologischeskaya kharakteristika mezozoyskikh otlozheniy yozhnoy chasti shelfa Barentseva morya (Palynological characterisation of the Mesozoic deposits of the southern Barents Sea Shelf). In *Stratigrafiya i paleontologiya Mesozoyskikh osadochnykh basseynov severa SSSR (Stratigraphy and Palaeontology of Mesozoic Sedimentary Basins of Northern USSR)* (ed. ND Vasilevskaya), pp. 88–103. PGO Sevmorgeologiya, Leningrad [in Russian].

Pott C (2014) The Upper Triassic flora of Svalbard. *Acta Palaeontologica Polonica* **59** (3), 709–40.

Rao AR (1943) Jurassic spores and sporangia from Rajmahal Hills, Bihar. *Proceedings of the National Academy of Sciences, India* **13B**, 181–97.

Reinhardt P (1962) Sporae dispersae aus dem Rhät Thüringens. *Monatsberichte der Deutschen Akademie der Wissenschaften zu Berlin* **3** (11/12), 704–11 [in German].

Retallack GJ (1975) The life and times of a Triassic lycopods. *Alcheringa* **1**, 3–29.

Retallack GJ (1997) Earliest Triassic origin of Isoetes and quillwort evolutionary radiation. *Journal of Paleontology* **71** (3), 500–21.

Riis F, Lundschien BA, Høy T, Mørk A and Mørk MBE (2008) Evolution of the Triassic shelf in the northern Barents Sea region. *Polar Research* **27**, 298–317.

Rismyhr B, Bjærke T, Olaussen S, Mulrooney MJ and Senger K (2018) Facies, palynostratigraphy and sequence stratigraphy of the Wilhelmøya Subgroup (Upper Triassic–Middle Jurassic) in western central Spitsbergen, Svalbard. *Norwegian Journal of Geology* **99**, 35–64. https://doi.org/10.17850/njg001

Roghi G, Gianolla P, Minarelli L, Pilati C and Preto N (2010) Palynological correlation of Carnian humid pulses throughout western Tethys. *Palaeogeography, Palaeoclimatology, Palaeoecology* **290**, 89–106.

Rossi VM, Paterson NW, Helland-Hansen W, Klausen TG and Eide CH (2019) Mud-rich delta-scale compound clinoforms in the Triassic shelf of northern Pangea (Havert Formation, south-western Barents Sea). *Sedimentology* **66** (6), 2234–2267. published online 9 March 2019, https://doi.org/10.1111/sed.12598

Ruffell AH, Simms MJ and Wignall PB (2015) The Carnian Humid Episode of the late Triassic: a review. *Geological Magazine* **153**, 271–84.

Ryseth A (2014) Sedimentation at the Triassic–Jurassic boundary, south-west Barents Sea: indication of climatic change. In *From Depositional Systems to Sedimentary Successions on the Norwegian Continental Margin* (eds AW Martinius, R Ravnås, JA Howell, RJ Steel and JP Wonham), pp. 187–214, Wiley-Blackwell: Oxford. International Association of Sedimentary Sedimentologists, Special Publication no. **46**.

Scheuring BW (1970) Palynologische und palynostratigraphische Untersuchungen des Keupers im Bölchentunnel (Solothurner Jura). *Schweizerische Paläontologische Abhandlungen Mémoires suisses de Paléontologie* **88**, 1–119, 43 plates [in German].

Schulz E (1967) Sporenpaläontologische Untersuchungen rätoliassischer Schichten im Zentralteil des Germanischen Beckens. *Paläontologische Abhandlungen Abteilung B* **2** (3), 543–633.

Schuurman WML (1977) Aspects of late Triassic palynology: 2. Palynology of the "Grès et Schiste à Avicula contorta" and "Argiles de Levallois" (Rhaetian) of north-eastern France and southern Luxemburg. *Review of Palaeobotany and Palynology* **23**, 159–253.

Schuurman WML (1979) Aspects of Late Triassic palynology. 3. Palynology of latest Triassic and earliest Jurassic deposits of the northern Limestone Alps in Austria and southern Germany, with special reference to a palynological characterization of the Rhaetian Stage in Europe. *Review of Palaeobotany and Palynology* **2**, 53–75.

Simms MJ and Ruffell AH (1989) Synchroneity of climatic change and extinctions in the late Triassic. *Geology* **17**, 265–68.

Simms MJ and Ruffell AH (2018) The Carnian Pluvial Episode: from discovery, through obscurity, to acceptance. *Journal of the Geological Society* **175** (6), 989–92.

Simms MJ, Ruffell AH & Johnson ALA (1994) Biotic and climatic changes in the Carnian (Triassic) of Europe and adjacent areas. In *In the Shadow of the Dinosaurs: Early Mesozoic Tetrapods* (eds NC Fraser and H-D Sues), pp. 352–65, Cambridge University Press, Cambridge.

Sivak J and Shang YK (1989) Discovery of new species of Kyrtomisporis in the Upper Trias (Norian and Rhaetian) of the Huobachong Formation in China. *Acta Palynologica* **1**, 49–90.

Smelror M Larssen GB, Olaussen S, Rømuld A and Williams R (2019) Late Triassic to Early Cretaceous palynostratigraphy of Kong Karls Land, Svalbard, Arctic Norway, with correlations to Franz Josef Land, Arctic Russia. *Norwegian Journal of Geology* **98** (4), 1–31.

Smith DG (1974) Late Triassic pollen and spores from the Kapp Toscana Formation, Hopen, Svalbard – a preliminary account. *Review of Palaeobotany and Palynology* **17**, 175–78.

Smith DG (1982) Stratigraphic significance of a palynoflora from ammonoid-bearing Early Norian strata in Svalbard. *Newsletters on Stratigraphy* **11** (3), 154–61.

Smith DG, Harland WB and Hughes NF (1975) Geology of Hopen, Svalbard. *Geological Magazine* **112** (1), 1–23.

Sømme TO, Doré AG, Lundin ER and Tørudbakken BO (2018) Triassic–Paleogene paleogeography of the Arctic: Implications for sediment routing and basin fill. *AAPG Bulletin* **102** (12), 2481–517.

Taylor TN, Taylor EL and Krings M (2009) *Paleobotany: The Biology and Evolution of Fossil Plants*, 2nd edn. Academic Press, Burlington, MA, 1230 pp.

Turland NJ, Wiersema JH, Barrie FR, Greuter W, Hawksworth DL, Herendeen PS, Knapp S, Kusber W-H, Li D-Z, Marhold K, May TW, McNeill J, Monro AM, Prado J, Price MJ and Smith GF (eds) (2018) International Code of Nomenclature for Algae, Fungi, and Plants (Shenzhen Code) Adopted by the Nineteenth International Botanical Congress Shenzhen, China, July 2017. Regnum Vegetabile, 159. Glashütten: Koeltz Botanical Books.

Van der Eem JGLA (1983) Aspects of Middle and Late Triassic palynology. 6. Palynological investigations in the Ladinian and lower Carnian of the Western Dolomites, Italy. *Review of Palaeobotany and Palynology* **39**, 189–300.

van Veen PM (1985) Stratigraphy of the Triassic in the Troms Area. Rapport, Oljedirektoratet, OD-85-36, 1–125.

Vasilevskaya ND (1972) The Late Triassic flora of Svalbard [in Russian]. In Mezozojskie otloženiâ Sval'barda (eds VN Sokolova and ND Vasilevskaya), 27–63. Naučno-Issledovatel'skij Institut Geologii Arktiki (NIIGA), Leningrad [in Russian].

Vigran JO, Mangerud G, Mørk A, Bugge T and Weitschat W (1998) Biostratigraphy and sequence stratigraphy of the Lower and Middle Triassic deposits from the Svalis Dome, Central Barents Sea, Norway. *Palynology* **22**, 89–141.

Vigran JO, Mangerud G, Mørk A, Worsley D and Hochuli PA (2014) *Palynology and geology of the Triassic succession of Svalbard and the Barents Sea*. Geological Survey of Norway, Special Publication no. **14**, 247 pp.

Weitschat W and Dagys A (1989) Triassic biostratigraphy of Svalbard and comparison of northeast Siberia. *Mitteilungen, Geologisch-Paläontologisches Institut der Universität Hamburg* **68**, 179–213.

Wood GD and Benson DG Jr (2000) The North American occurrence of the algal coenobium Plaesiodictyon: paleogeographic, paleoecologic, and biostratigraphic importance in the Triassic. *Palynology* **24**, 9–20.

Wood GD and Miller MA (1998) Stratigraphic, paleoecologic and petroleum generating significance of Chlorophyta (chlorococcalean algae) in the Cretaceous of Western Africa and South America. *African Geoscience Review* **4**, 499–510.

Xu G, Hannah JL, Stein HJ, Bingen B, Yang G, Zimmermann A, Weitschat W, Mørk A and Weiss HM (2009) Re-Os geochronology of Arctic black shales to evaluate the Anisian – Ladinian boundary and global fauna correlations. *Earth and Planetary Science Letters* **288**, 581–87.

Xu G, Hannah JL, Stein HJ, Mørk A, Vigran JO, Bingen B, Schutt DL and Lundschien A (2014) Cause of Upper Triassic climate crisis revealed by Re-Os geochemistry of Boreal black shales. *Palaeogeography, Palaeoclimatology, Palaeoecology* **395**, 222–32.

https://doi.org/10.1017/S0016756819000906 Published online by Cambridge University Press